

Multistage Antiplasmodium Activity of Astemizole Analogues and Inhibition of Hemozoin Formation as a Contributor to Their Mode of Action

Malkeet Kumar, John Okombo, Dickson Mambwe, Dale Taylor, Nina Lawrence, Janette Reader, Mariëtte van der Watt, Diana Fontinha, Margarida Sanches-Vaz, Belinda C Bezuidenhout, Sonja Lauterbach, Dale Liebenberg, Lyn-Marie Birkholtz, Theresa L. Coetzer, Miguel Prudêncio, Timothy J Egan, Sergio Wittlin, and Kelly Chibale

ACS Infect. Dis., **Just Accepted Manuscript** • DOI: 10.1021/acsinfecdis.8b00272 • Publication Date (Web): 11 Dec 2018

Downloaded from <http://pubs.acs.org> on December 15, 2018

Just Accepted

“Just Accepted” manuscripts have been peer-reviewed and accepted for publication. They are posted online prior to technical editing, formatting for publication and author proofing. The American Chemical Society provides “Just Accepted” as a service to the research community to expedite the dissemination of scientific material as soon as possible after acceptance. “Just Accepted” manuscripts appear in full in PDF format accompanied by an HTML abstract. “Just Accepted” manuscripts have been fully peer reviewed, but should not be considered the official version of record. They are citable by the Digital Object Identifier (DOI®). “Just Accepted” is an optional service offered to authors. Therefore, the “Just Accepted” Web site may not include all articles that will be published in the journal. After a manuscript is technically edited and formatted, it will be removed from the “Just Accepted” Web site and published as an ASAP article. Note that technical editing may introduce minor changes to the manuscript text and/or graphics which could affect content, and all legal disclaimers and ethical guidelines that apply to the journal pertain. ACS cannot be held responsible for errors or consequences arising from the use of information contained in these “Just Accepted” manuscripts.



Multistage Antiplasmodium Activity of Astemizole Analogues and Inhibition of Hemozoin Formation as a Contributor to Their Mode of Action

Malkeet Kumar¹, John Okombo¹, Dickson Mambwe¹, Dale Taylor², Nina Lawrence², Janette Reader³, Mariëtte van der Watt³, Diana Fontinha⁴, Margarida Sanches-Vaz⁴, Belinda C Bezuidenhout⁵, Sonja B Lauterbach⁵, Dale Liebenberg⁵, Lyn-Marie Birkholtz³, Theresa L Coetzer⁵, Miguel Prudêncio⁴, Timothy J. Egan^{1,6}, Sergio Wittlin^{7,8}, Kelly Chibale^{1,6,9}*

¹Department of Chemistry, University of Cape Town, Rondebosch 7701, South Africa.

²Drug Discovery and Development Centre (H3D), Division of Clinical Pharmacology, Department of Medicine, University of Cape Town, Observatory 7925, South Africa.

³Department of Biochemistry, Genetics and Microbiology, Institute for Sustainable Malaria Control, University of Pretoria, Private Bag X20, Hatfield 0028, South Africa.

⁴Instituto de Medicina Molecular, Faculdade de Medicina, Universidade de Lisboa, Av. Prof. Egas Moniz, 1649-028 Lisboa, Portugal.

⁵Department of Molecular Medicine and Haematology, School of Pathology, Faculty of Health Sciences, University of the Witwatersrand and National Health Laboratory Service, Johannesburg 2193, South Africa

⁶Institute of Infectious Disease and Molecular Medicine, University of Cape Town, Rondebosch 7701, South Africa.

⁷Swiss Tropical and Public Health Institute, Socinstrasse 57, 4002 Basel, Switzerland

⁸University of Basel, 4003 Basel, Switzerland.

⁹South African Medical Research Council Drug Discovery and Development Research Unit, Department of Chemistry University of Cape Town, Rondebosch 7701, South Africa.

1
2
3 *Corresponding Author: Kelly Chibale
4

5 Email: Kelly.Chibale@uct.ac.za: Phone: +27-21-6502553. Fax: +27-21-6505195.
6
7
8
9

10 A drug repositioning approach was leveraged to derivatize astemizole (AST), an antihistamine
11 drug whose antimalarial activity was previously identified in a high-throughput screen. The
12 multistage activity potential against *Plasmodium* parasite's life cycle of the subsequent analogues
13 was examined by evaluating against the parasite asexual blood, liver and gametocyte stages. In
14 addition, the previously reported contribution of heme detoxification to the compound's mode of
15 action was interrogated. Ten of the seventeen derivatives showed $IC_{50}s < 0.1 \mu M$ against the
16 chloroquine (CQ)-sensitive *Plasmodium falciparum* NF54 (*Pf*NF54) strain while maintaining
17 submicromolar potency against the multidrug resistant strain, *Pf*K1, with most showing low
18 likelihood of cross-resistance with CQ. Selected analogues (*Pf*NF54- $IC_{50} < 0.1 \mu M$) were tested
19 for cytotoxicity on CHO cells and found to be highly selective (selectivity index > 100). The first
20 ever gametocytes screening of AST and its analogues revealed their moderate activity (IC_{50} : 1 – 5
21 μM) against late stage *P. falciparum* gametocytes, while the evaluation of activity against *P.*
22 *berghei* liver stages identified one compound (**3**) with three-fold greater activity than the parent
23 AST compound. Mechanistic studies showed a strong correlation between *in vitro* inhibition of β -
24 haematin formation by the AST derivatives and their antiplasmodium $IC_{50}s$. Analyses of
25 intracellular inhibition of hemozoin formation within the parasite further yielded signatures
26 attributable to a possible perturbation of the heme detoxification machinery.
27
28
29
30
31
32
33
34
35
36
37
38
39
40
41
42
43
44
45
46
47
48
49

50 **Key Words:** Astemizole, Repositioning, *Plasmodium falciparum*, β -haematin, Gametocytes
51
52
53
54
55
56
57
58
59
60

1
2
3
4
5
6
7
8
9
10 The latest statistics from the World Health Organization estimate that there were 216 million cases
11 and 445,000 deaths due to malaria in 2016.¹ While these numbers mirror a trend of declining
12 malaria burden over the past 15 years due to control strategies, which comprise indoor residual
13 spraying, insecticide-treated nets, intermittent preventive treatments and adoption of artemisinin
14 combinations as first-line therapy, the disease still remains a major public health concern. In fact,
15 the recent evolution and dissemination of artemisinin-tolerant *Plasmodium falciparum* strains and
16 suboptimal response to insecticides used for management of the *Anopheles* vector threaten the
17 ultimate success of these control efforts.^{2,3} To minimize the likelihood of rapid development of
18 drug resistance, there is a clear need for innovation in order to identify safe and effective
19 antimalarial compounds that can preferably inhibit multiple stages of the parasite's life cycle,
20 which includes the asexual erythrocytic blood stage, the transmissible sexual gametocytic stage
21 and a hepatocytic liver stage . One attractive approach to novel antimalarial drug design that can
22 significantly reduce the pitfalls inherent to drug development is the repositioning of already-
23 approved pharmacotherapies – a strategy whose application in malaria and neglected tropical
24 diseases has been reviewed elsewhere.⁴

25
26
27
28
29
30
31
32
33
34
35
36
37
38
39
40
41
42
43
44
45 In the search for new drugs to treat malaria, researchers at Johns Hopkins University (JHU), in
46 2006, screened a chemical library comprising 2 687 Food and Drug Administration (FDA)-
47 approved drugs for potential inhibitors of *P. falciparum* proliferation. This led to the discovery of
48 antiplasmodium properties of astemizole (AST) (**Figure 1**), a second-generation antihistamine,
49 which was withdrawn from market due to cardiotoxicity caused by its hERG channel blocking
50
51
52
53
54
55
56
57
58
59
60

activity and association with arrhythmias.⁵ In that study, AST exhibited submicromolar half-maximal inhibitory concentrations (IC₅₀s) against three *P. falciparum* strains with different levels of chloroquine (CQ) sensitivity.⁵ In humans, AST is rapidly absorbed from the gastrointestinal tract and undergoes extensive first-pass metabolism to the pharmacologically active desmethylastemizole (DM-AST) and other minor metabolites, including nor-astemizole (Nor-AST) (**Figure 1**).⁶ Incidentally, these metabolites also exhibited antiplasmodium activity in the JHU screen, with DM-AST showing two- to twelve-fold higher potency than AST, depending on the parasite strain (**Figure 1**).⁵ Further evaluation revealed their antimalarial potential, with 80% and 81% suppression of parasitaemia in *P. vinckei*-infected mice treated for four days with AST (30 mg/m²/day) and DM-AST (15 mg/m²/day), respectively.⁵

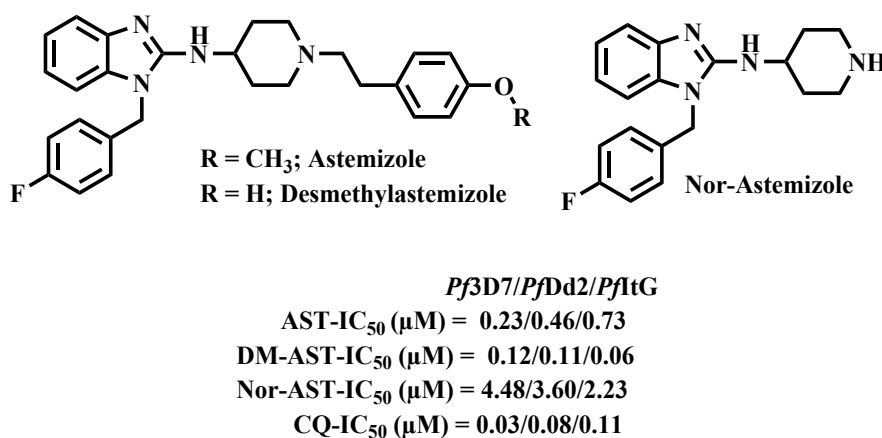


Figure 1: Chemical structures and antiplasmodium activity of AST and its metabolites as reported by Chong *et al* (2006) against *Pf3D7*, *PfDd2* and *PfItG* strains.⁵

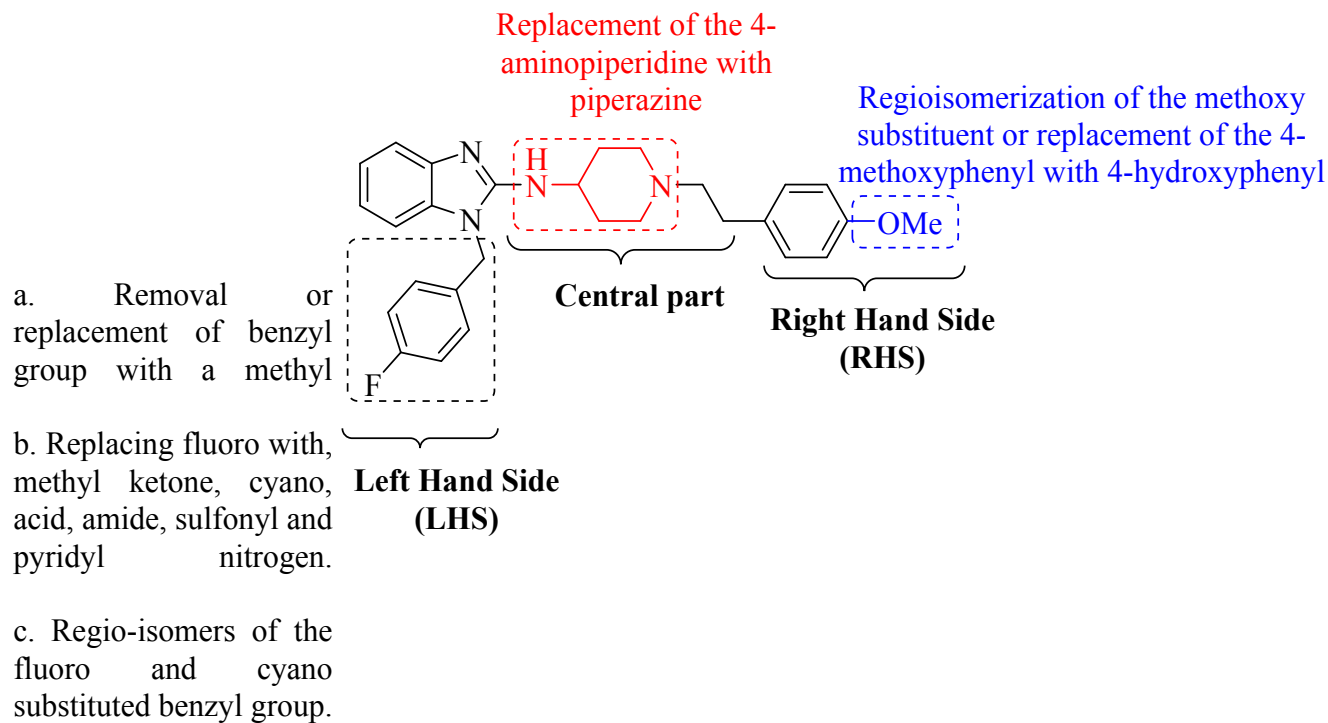
Encouragingly, the antimalarial potential of AST has been recently investigated by other researchers. Employing a conjugated approach that hybridized CQ and AST structural motifs, Musonda *et al.* reported on CQ-AST hybrid compounds with *in vitro* activity against CQ-resistant (CQR) strains and *in vivo* activity in a murine malaria model.⁷ Similarly, Roman and colleagues

1
2
3 reported on potent AST derivatives bearing several modifications to the AST structure against the
4 CQR *P. falciparum* strain, ItG.⁸ More recently, Tian and co-workers identified AST derivatives
5 that showed good activity against the CQS strain, *Pf3D7*, and exhibited reduced hERG channel
6 inhibition potency.⁹ Various known chemical modification strategies can be employed to mitigate
7 hERG channel inhibition activity in new AST analogues. These include (a) reduction of
8 lipophilicity *via* removal of aromatic groups as already demonstrated in case of AST⁹, reduction
9 in the clogP *via* incorporation of polar moieties and heteroaromatic replacement of aromatic
10 groups; (b) attenuation of pKa *via* modulation of the basicity of a nitrogen atom; (c) incorporation
11 of three dimensional character and reduction in π - π stacking interactions. While these studies
12 focused solely on the inhibition of asexual blood stage parasite proliferation, Derbyshire and co-
13 workers further reported on the effectiveness of AST in a high-throughput phenotypic screen
14 developed to systematically identify molecules with liver-stage efficacy.¹⁰

15
16
17
18
19
20
21
22
23
24
25
26
27
28
29
30
31 The basic premise of the drug repositioning approach involves further re-engineering of the
32 original molecule for optimization into a new chemical entity with improved potency,
33 physicochemical profile and/or safety. Although, the findings from the seminal JHU screen have
34 been pursued by others to highlight the antimalarial potential of AST, to our knowledge no
35 medicinal chemistry effort to date has focused on probing the multistage antiplasmodium activity
36 of AST analogues across liver, asexual blood and gametocytic life-cycle stages. As an extension
37 to our group's efforts aimed at identifying multistage active antiplasmodium compounds, this
38 article explores structural modifications around the core AST pharmacophore (**Figure 2**) in
39 anticipation of developing analogues with favourable solubility and cytotoxicity indices, as well
40 as activity against different stages of the parasite's life cycle. This involved i) amending the central
41 part of AST through replacement of the 4-aminopiperidine moiety with a piperazine; ii) modifying
42
43
44
45
46
47
48
49
50
51
52
53
54
55
56
57
58
59
60

1
2
3 the left hand side (LHS) of AST by a) complete removal of the benzyl group and replacing it with
4 a methyl or b) replacing the fluoro moiety with, methyl ketone, cyano, acid, amide, sulfonyl and
5 pyridyl nitrogen or c) regio-isomers of the fluoro- and cyano-substituted benzyl group; and iii)
6 regio-isomerization of the methoxy substituent or replacement of the 4-methoxyphenyl with 4-
7 hydroxyphenyl on the right hand side (RHS) of AST. Some of the analogues with modifications
8 on LHS of AST such as complete removal of the benzyl group and its replacement with a methyl
9 group as well as replacement of fluoro substituent on benzyl moiety with amide, sulfonyl, acid and
10 pyridyl groups were also aimed at reducing lipophilicity (cLogP < 4.5 vs AST cLogP of 5.84;
11 Supplementary Information Table S1).

12
13
14
15
16
17
18
19
20
21
22
23
24
25 During *Plasmodium* blood stage infection, host haemoglobin (Hb) is degraded into globin as a
26 nutrient source, and heme is released as a by-product of this obligate catabolism. However, in its
27 free state, heme is toxic as it can induce free radical formation as well as membrane damage.^{11,12}
28
29 To bypass this toxicity, *P. falciparum* converts heme into insoluble hemozoin (Hz) crystals - a
30 detoxification process known to be inhibited by quinolines such as CQ and one that is tractable
31 using *in vitro* models which mimic the digestive vacuole (DV) milieu. In line with previous
32 findings showing that AST and DM-AST concentrate within the parasite's DV, inhibit heme
33 crystallization and co-purify with Hz in drug-sensitive and resistant parasites,⁵ we also queried the
34 contribution of inhibition of heme detoxification as at least one of the possible modes of action
35 (MoA) of AST.
36
37
38
39
40
41
42
43
44
45
46
47
48
49
50
51
52
53
54
55
56
57
58
59
60



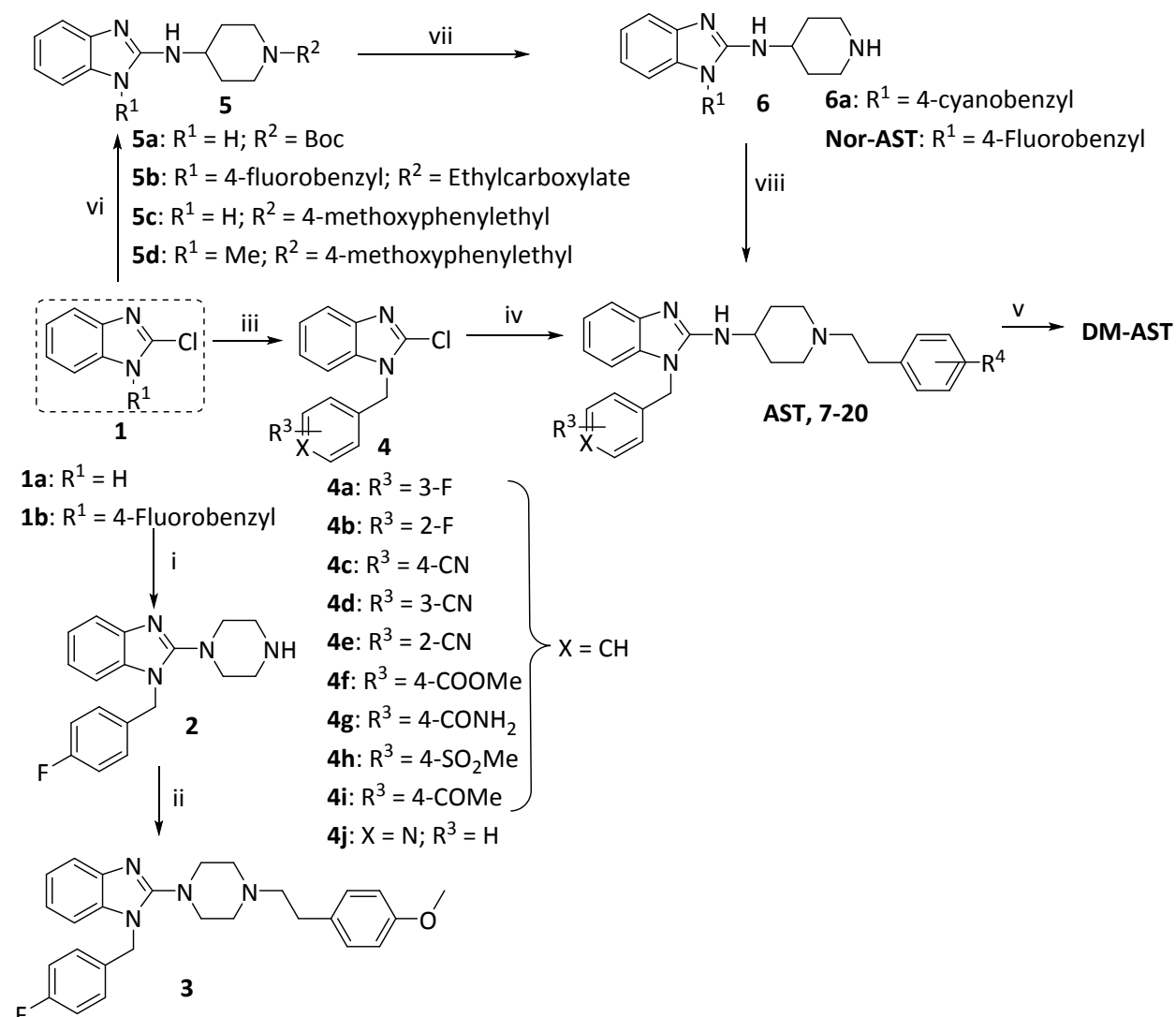
26 **Figure 2:** Structural modifications around AST to design various derivatives

27
28
29
30
31
32
33
34
35 **CHEMISTRY:** The synthesis of AST analogues is summarized in **Scheme 1**. AST analogue **3**
36 with the piperazinyl moiety replacing AST's amino piperidinyl moiety was synthesized in two
37 steps, a reaction of commercially available **1b** with piperazine followed by 1-(2-bromoethyl)-4-
38 methoxybenzene. The synthesis of compounds **7-16** commenced with the benzylation of
39 commercially available 2-chlorobenzimidazole (**1a**) using K_2CO_3 in acetone to afford
40 intermediates **4a-j**, which were subsequently reacted with 1-(4-methoxyphenethyl)piperidin-4-
41 amine in a neat reaction at 170 °C to obtain AST analogues **7-16**. AST was obtained by direct
42 reaction of **1b** with 1-(4-methoxyphenethyl)piperidin-4-amine while the demethylation of AST
43 using HBr afforded DM-AST.
44
45
46
47
48
49
50
51
52
53
54
55
56
57
58
59
60

1
2
3 The synthesis of compounds **17-20** began with the reaction of **1a, b** with protected
4 4-aminopiperidines to afford intermediate **5a, b** (Scheme 1). The benzylation of **5a** with 4-
5 (bromomethyl)benzotrile followed by deprotection using 4M HCl in dioxane afforded **6a**, while
6
7
8 Nor-AST was obtained by direct deprotection of **5b**. The reaction of **6a** and Nor-AST with the
9
10
11
12
13
14
15
16
17
18
19
20
21
22
23
24
25
26
27
28
29
30
31
32
33
34
35
36
37
38
39
40
41
42
43
44
45
46
47
48
49
50
51
52
53
54
55
56
57
58
59
60

respective phenyl ethyl bromide using K₂CO₃ in acetonitrile at reflux resulted in compounds **17-20** (Scheme 1). The AST analogue **5c** was obtained by direct reaction of **1a** with 1-(4-methoxyphenethyl)piperidin-4-amine. On the other hand, **1a** was first *N*-methylated and then reacted with 1-(4-methoxyphenethyl)piperidin-4-amine to afford analogue **5d**.

Scheme 1: Synthesis of AST analogues



Reagents and conditions: (i) **1b**, piperazine, Et₃N, *t*-BuOH, 120 °C, 48 h, 87%; (ii) 1-(2-bromoethyl)-4-methoxybenzene, toluene, reflux, 48 h, 50%; (iii) **1a**, appropriate benzyl halide, K₂CO₃, acetone, 23 °C, 4-6 h, 70-85% (**4a-j**); (iv) 1-(4-methoxyphenethyl)piperidin-4-amine, 170 °C, 6-12 h, 15-74% (AST, **7-16**); (v) AST, HBr, reflux (120 °C), 6 h, 48%; (vi) **1a**, 4-amino-N-boc-piperidine, TEA, 150 °C, 2 h, 60% (**5a**); **1b**, ethyl 4-aminopiperidine-1-carboxylate, 170 °C, 4 h, 98% (**5b**); 1-(4-methoxyphenethyl)piperidin-4-amine, 170 °C, 4 h, 48% (**5c**); (a) **1a**, methyl iodide, K₂CO₃, acetone, 23 °C, 30 min, 68%; (b) 1-(4-methoxyphenethyl)piperidin-4-amine, 170

1
2
3 °C, 8 h, 30% (**5d**); (vii) (a) **5a**, 4-(2-bromomethyl)benzotrile, K₂CO₃, DMF, 70 °C, 3 h, 88%;
4
5 (b) 4N HCl in dioxane, 18 °C, 2 h, 80% (**6a**); **5b**, HBr, reflux (120 °C), 6 h, 85% (Nor-AST);
6
7 (viii) **6a**, 4-(2-bromoethyl)phenol, K₂CO₃, ACN, 79 °C, reflux (85 °C), 5 h, 36%; (**17**); Nor-AST,
8
9 1-(2-bromoethyl)-3-methoxybenzene, ACN, reflux (85 °C), 16 h, 78% (**18**); Nor-AST, 1-(2-
10
11 bromoethyl)-2-methoxybenzene, ACN, reflux (85 °C), 24 h, 71% (**19**); Nor-AST, (2-
12
13 bromoethyl)benzene, ACN, reflux (85 °C), 12 h, 79% (**20**).
14
15
16
17

18 RESULTS & DISCUSSION:

19 Blood Stage Antiplasmodium Activity, Cytotoxicity and Solubility:

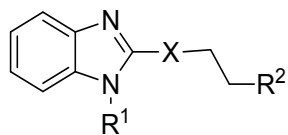
20
21 The antiplasmodium activity of AST, DM-AST, Nor-AST and all newly synthesized analogues
22
23 was evaluated against the CQ sensitive *Pf*NF54 strain. Compounds with sub-micromolar potency
24
25 against *Pf*NF54 were further tested against the multidrug resistant *Pf*K1 strain. Additionally,
26
27 solubility of all the compounds was determined while analogues with IC₅₀ ≤ 0.1 μM against
28
29 *Pf*NF54 were also tested for cellular toxicity against CHO cells (**Table 1**).
30
31
32
33

34
35 Replacing the amino piperidine in the central core of the AST structure with piperazine (**3**) did not
36
37 increase antiplasmodium activity (*Pf*NF54-IC₅₀ = 1.9 μM), as the resulting compound exhibited
38
39 comparably less activity than AST (*Pf*NF54-IC₅₀ = 0.086 μM). The structural changes on the LHS
40
41 of the molecule showed that the benzyl group is not important for the activity, as the debenzylated
42
43 analogue **5c** (*Pf*NF54-IC₅₀ = 0.047 μM) showed enhanced activity compared to AST. However,
44
45 methylation of the benzimidazole nitrogen (**5d**) led to a 7.5-fold reduction in activity (*Pf*NF54-
46
47 IC₅₀ = 0.35 μM) as compared to **5c** (*Pf*NF54-IC₅₀ = 0.047 μM), demonstrating the plausible
48
49 contribution of the free benzimidazole nitrogen towards the potency of **5c**. Additionally, the
50
51 antiplasmodium activity of **5c** (*Pf*K1-IC₅₀ = 1.7 μM) was ablated in the *Pf*K1 drug-resistant strain
52
53
54
55
56
57
58
59
60

($PfK1-IC_{50} = 1.7 \mu M$), and this compound showed a high propensity for cross-resistance with CQ (RI = 35). Regarding the substituents replacing the 4-fluoro group on the benzyl motif, electron withdrawing substituents such as cyano (**9**; $PfNF54-IC_{50} = 0.078 \mu M$), sulfonyl (**14**; $PfNF54-IC_{50} = 0.23 \mu M$) and methyl ketone (**15**; $PfNF54-IC_{50} = 0.12 \mu M$) were tolerated and showed comparable activity to AST. On the other hand, amide (**13**; $PfNF54-IC_{50} = 0.41 \mu M$), acid (**12**; $PfNF54-IC_{50} = 1.5 \mu M$) and pyridyl (**16**; $PfNF54-IC_{50} = 1.7 \mu M$) replacements reduced potency approximately by five-, seventeen- and nineteen-fold, respectively. The fluoro (**7**; $PfNF54-IC_{50} = 0.068 \mu M$, and **8**; $PfNF54-IC_{50} = 0.075 \mu M$) and two of the cyano (**9**; $PfNF54-IC_{50} = 0.078 \mu M$, and **10**; $PfNF54-IC_{50} = 0.055 \mu M$) regio-isomers showed comparable activity to AST, while the 2-cyano analogue (**11**; $PfNF54-IC_{50} = 0.033 \mu M$) showed more than two-fold enhanced potency compared to AST. This demonstrated that substituent positional change on the benzyl group is tolerated and may deliver compounds with enhanced potency.

Regarding changes to the RHS, the DM-AST congener, **17**, bearing a 4-cyano benzyl group was three-fold more potent than AST ($PfNF54-IC_{50} = 0.086 \mu M$) and showed slightly better activity than DM-AST ($PfNF54-IC_{50} = 0.04 \mu M$ vs $0.028 \mu M$). The methoxy regio-isomers **18** ($PfNF54-IC_{50} = 0.089 \mu M$), **19** ($PfNF54-IC_{50} = 0.077 \mu M$) and the unsubstituted derivative **20** ($PfNF54-IC_{50} = 0.089 \mu M$) were equipotent and had comparable activity to AST.

A selected number of analogues (**5c**, **7-11** and **18-20**; $PfNF54-IC_{50} \leq 0.1 \mu M$) were advanced for evaluation of cytotoxicity in CHO cells, exhibiting high selectivity indices (selectivity index, SI > 100; **Table 1**). All the analogues except **11** and **15** also exhibited generally good aqueous solubility (**Supplementary Information Table S1**). There was no discernible improvement in solubility among the derivatives relative to AST, except when the benzyl on the LHS of the molecule was replaced with a methyl group (**5d**; $155 \mu M$).

Table 1: Antiplasmodium activity and cytotoxicity of AST and the synthesized analogues.

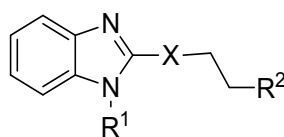
Compound	R ¹	X	R ²	Antiplasmodium			Cytotoxicity	
				Activity IC ₅₀			CHO ^d IC ₅₀	
				(μM) ^{a,b}			(μM)	
				<i>Pf</i> NF54	<i>Pf</i> K1	R.I. ^c		
AST				0.086	0.37	4.3	29.6	344
DM-AST				0.040	0.03	0.8	23.0	575
Nor-AST			----	1.1	0.92	0.8	--	--
3				1.9	-	-	--	--
5c	H			0.047	1.7	36.2	40.4	860
5d	H ₃ C			0.35	2.2	6.3	--	--
7				0.068	0.31	4.6	43.8	644
8				0.075	0.34	4.5	40.4	539
9				0.078	0.36	4.6	21.2	272
10				0.055	0.33	6.0	39.7	722
11				0.033	0.18	5.5	43.6	1321
12				1.5	-	-	--	--

Compound	R ¹	X	R ²	Antiplasmodium			Cytotoxicity	
				Activity IC ₅₀			CHO ^d IC ₅₀	
				(μM) ^{a,b}			(μM)	S.I. ^e
				<i>Pf</i> NF54	<i>Pf</i> K1	R.I. ^c		
13				0.41	2.2	5.4	--	--
14				0.23	1.3	5.7	--	--
15				0.12	0.43	3.6	--	--
16				1.7	--	--	--	--
17				0.028	0.041	1.5	38.5	1376
18				0.089	0.43	4.8	41.0	461
19				0.077	0.32	4.2	43.1	560
20				0.086	0.37	4.3	32.4	377
Chloroquine				0.004	0.14	35.0	--	--
Artesunate				0.003	0.001	0.3	--	--
Emetine							0.95	

^aAll the *in vitro* antiplasmodium testing was performed in Modified [³H]-hypoxanthine incorporation assay at Swiss TPH except compounds **16** and **17** which were evaluated in parasite lactate dehydrogenase assay at UCT; ^bReadout is mean from two independent experiments (n = 2) for multidrug resistant (*Pf*K1) and CQ-sensitive (*Pf*NF54) strains of *P. falciparum*; ^cRI = Resistance Index (*Pf*K1-IC₅₀/*Pf*NF54-IC₅₀); ^dCHO = Chinese hamster ovarian cells; ^eSI = Selectivity Index (CHO IC₅₀/*Pf*NF54-IC₅₀).

Gametocyte and Liver Stage Activity: While the ability of AST to inhibit proliferation of *P. berghei* liver stage parasites has been documented,¹⁰ there are no reports on the gametocytocidal potential of this class of compounds. We therefore tested AST, DM-AST and nine other AST analogues (**3**, **5c**, **10**, **11**, **14**, **15** and **18-20**) against late (LG; > 95% stage IV/V) gametocytes. Only two analogues showed activity, with **5c** ($IC_{50} = 1.9 \mu M$) being the most potent against late stage gametocytes compared to AST ($IC_{50} = 3.4 \mu M$) and **18** ($IC_{50} = 4.1 \mu M$) (**Table 2**). None of the compounds showed improved activity against early stage gametocytes (> 90% stage II/III) compared to AST (data not shown). To the best of our knowledge, this data represents the first evidence of activity of AST and its derivatives against gametocytes.

Table 2: Gametocyte and liver stage activity of AST and analogues:



Compound	R ¹	X	R ²	IC ₅₀ (μM)			Cell confluency (% of control)
				^a Late gametocyte stage	^b Liver stage	Blood stage	
AST				3.4	0.66 ± 0.79	0.086	>73%
DM-AST				NS ^c	0.14 ± 0.031	0.04	>91%
3				NS ^c	0.21 ± 0.12	1.9	>91%
5c	H			1.9	NS ^d	0.047	NS ^d
18				4.1	NS ^d	0.089	NS ^d
Primaquine					8.4		

1		
2		
3	MB	0.14
4		
5		0.00
6	Chloroquine	4
7		

^aLate gametocyte stage: Data was obtained in a single experiment (n = 1) as a technical triplicate; ^bLiver stage: Data represents the mean \pm SD of n = 3 independent experiments performed in triplicate obtained for inhibition of the infection of human hepatoma cells (Huh7) by *P. berghei*; NS^c: Not selected for IC₅₀ determination as they showed < 50% inhibition in an initial dual-point screen at 1 and 5 μ M; NS^d: Not selected for IC₅₀ determination due to < 50% reduction in liver stage parasite load at \leq 1.0 μ M concentration; MB = methylene blue.

The potential for inhibition of liver stage infection was probed using a model of *P. berghei*-infection of the Huh7 human hepatoma cell line.¹³ Preliminary screening for liver stage activity of AST, DM-AST, Nor-AST, **3**, **5c**, **7-15** and **17-20** at four different concentrations (10 μ M, 1 μ M, 0.1 μ M and 0.01 μ M) showed that only DM-AST and analogue **3** exhibited > 50% reduction of parasite load at \leq 1 μ M with IC₅₀ values of 0.14 μ M and 0.21 μ M, respectively (**Table 2**). In parallel, Huh7 cell confluency was assessed in the presence of each compound concentration, as a measurement of cytotoxicity (Table 2). The activity of AST in our analysis was, however, lower than reported by Derbyshire *et al* (AST: IC₅₀ = 0.114 μ M),¹⁰ which might result from the fact that different cell lines were employed in two protocols (HepG2 versus HuH7) or from distinct varying cell densities in each assay.¹⁰

Mechanistic Studies: In humans, AST competitively binds to histamine H₁ receptor sites.¹⁴ Although Chong and colleagues implicated the inhibition of heme crystallization within the parasite in AST's activity, the drug's exact MoA in *Plasmodium* is yet to be established.⁵ Employing a pyridine-based, detergent-mediated *in vitro* model that partially recapitulates the micro-environment within the DV and quantifies the inhibition of formation of synthetic Hz, β -

1
2
3 haematin (β H),¹⁵ we assessed the ability of AST derivatives to block β H formation as surrogate
4 for the inhibition of heme detoxification by the parasite. Invoking a discriminatory IC_{50} of 100 μ M
5 to identify active inhibitors, four of the twenty evaluated compounds blocked β H formation, albeit
6 less potently than the standard β H formation inhibitors amodiaquine (IC_{50} : 11 μ M) and CQ (IC_{50} :
7 23 μ M) (**Supplementary Information Table S1**). Although inhibition was not directly linked to
8 any specific structural modification of AST, all the active derivatives comprised analogues bearing
9 nitrile or carboxylic acid substitution of the fluorine at the C4 position on the LHS phenyl ring.
10 Seeking possible structure-activity relationships, we observed a strong and significant positive
11 correlation ($R^2 = 0.6759$, $p < 0.0001$) between β H inhibition and activity against *Pf*NF54
12 (**Supplementary Information Figure S1**). As a caveat, we reiterate that this assay represents an
13 *in vitro* set-up with the attendant limitations of mimicking the physiological complexities of
14 intracellular drug activity, which include membrane permeation and vacuolar accumulation. These
15 data support inhibition of the heme detoxification pathway as a possible contributing mechanism
16 of the antiplasmodium action of the AST derivatives analysed in the present study.
17
18

19 To establish whether or not this series actually inhibits intracellular Hz formation in *P. falciparum*,
20 DM-AST and compound **10** (with β H inhibitory profiles) were progressed into a cellular heme
21 fractionation assay designed to delineate a dose-dependent effect of compounds on the various
22 heme species (Hb, free heme and Hz) in the parasite.¹⁶ Exposure of synchronized ring stage
23 *Pf*NF54 parasites to each of the two compounds for 32 h led to statistically significant
24 concentration-dependent increases in the proportions of free heme and a corresponding decrease
25 in Hz, similarly to what is observed for CQ (**Figure 3**). Indeed, this concentration-dependent
26 profile persisted for both derivatives when the analysis was focused on the amount of heme
27 (expressed as mass of heme Fe) measured per cell. Thus, these results, corroborate the findings of
28
29
30
31
32
33
34
35
36
37
38
39
40
41
42
43
44
45
46
47
48
49
50
51
52
53
54
55
56
57
58
59
60

Chong et al.,⁵ as they strongly suggest that inhibition of H_z formation is a likely, although not necessarily the only, potential MoA of these two AST analogues. Indeed, given the liver stage activity of DM-AST, there must be other targets, suggesting a possible pleiotropic mechanism, at least for this compound.

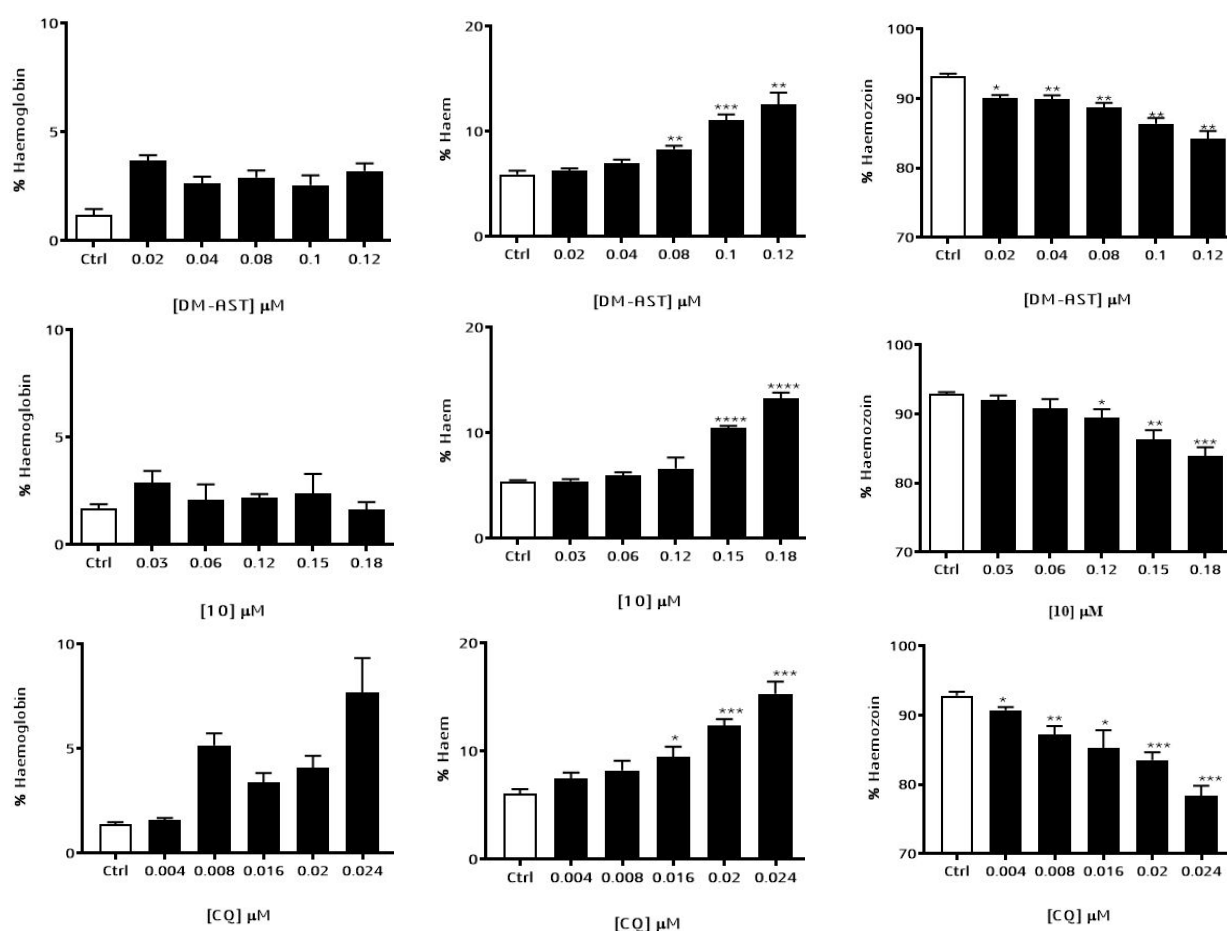


Figure 3: Dose-dependent effect of DM-AST, 10 and CQ on Hb (left panels), ‘free’ heme (middle panels), and Hz (right) panels in *PfNF54*. Significant increases in Hb and heme and decreases in Hz relative to the control were calculated using a two-tailed *t*-test and are denoted in asterisk: (*) $P < 0.05$; (**) $P < 0.01$; (***) $P < 0.001$.

CONCLUSION:

As follow up on earlier work on the antimalarial activity of AST, we have presented an investigation on the derivatization and evaluation of the cytotoxicity, activity against different stages of the parasite life cycle, and potential MoA of AST and seventeen analogues. Structural modifications of the AST pharmacophore showed that replacement of the 4-fluoro group on the LHS with a nitrile group was particularly favoured for blood stage activity, especially when accompanied by a hydroxyl substitution for the methoxy group on the RHS of the molecule. Appreciable activity against late stage gametocytes and liver stage parasites was also observed, thus introducing the possibility for optimization towards dual- or triple-action antimalarial agents. To this end, **5c** represents a promising starting point due to its good asexual blood and moderate sexual gametocyte stage activities while further optimization of **3** should be aimed at improving its asexual blood stage activity to match its good liver stage activity. In addition, our data confirm previous findings of the likely contribution of inhibition of heme detoxification as a contributing mechanism to the antiplasmodium effect of AST. Finally, the high selectivity observed for these molecules highlights their cellular safety, at least in lower mammals. Further optimization and evaluation of additional AST derivatives is thus warranted.

EXPERIMENTAL:

All commercially available chemicals were purchased from Sigma-Aldrich or Combi-Blocks, South Africa. All solvents were dried by appropriate techniques. Unless otherwise stated, all solvents used were anhydrous. ¹H-NMR and ¹³C-NMR spectra were recorded on Bruker spectrometer at 400 MHz (¹H 400.2 MHz; ¹³C 100.6 MHz) or Bruker-600 (¹H 600.3 MHz; ¹³C 150.9 MHz). Melting points were determined on a Lasec automatic melting point machine. Analytical thin-layer chromatography (TLC) was performed on aluminium-backed silica-gel 60

1
2
3 F₂₅₄ (70-230 mesh) plates with detection and visualization done using (a) UV lights (254/366 nm),
4
5 (b) iodine vapor and (c) ninhydrin spray reagent. Column chromatography was performed with
6
7 Merck silica-gel 60 (70-230 mesh). Chemical shifts (δ) are given in ppm downfield from TMS as
8
9 the internal standard. Coupling constants were recorded in Hertz (Hz). Purity was determined by
10
11 Agilent 1260 Infinity binary pump, Agilent 1260 Infinity diode array detector (DAD), Agilent
12
13 1290 Infinity column compartment, Agilent 1260 Infinity standard autosampler, and Agilent 6120
14
15 quadrupole (single) mass spectrometer, equipped with APCI and ESI multimode ionization source,
16
17 and all compounds tested for biological activity were confirmed to have $\geq 95\%$ purity. The HPLC
18
19 method used is described in material and method section. Any data not shown below is supplied
20
21 in the Supporting files.
22
23
24
25

26 27 **1-(4-fluorobenzyl)-2-(piperazin-1-yl)-1H-benzo[d]imidazole (2)**

28
29 A solution **1b** (0.2 grams, 0.071 mmol) and piperazine (0.66 grams, 0.71 mmol) in *t*-BuOH was
30
31 treated with triethyl amine (0.77 grams, 1.1 mL, 0.71 mmol). The resulting reaction mixture was
32
33 stirred at 120 °C in a closed vessel for 48 h. After the completion of reaction, reaction was
34
35 quenched with aqueous saturated solution of NaHCO₃ and extracted with ethyl acetate (4 × 10
36
37 mL). The combined organic layers were dried over sodium sulfate and concentrated *in vacuo* to
38
39 afford crude product. The recrystallization of crude product from a mixture of pentane and DCM
40
41 furnished pure compound **2** (0.2 grams, 87% yield). m.p. 107.9-108.9 °C; ¹H-NMR (400 Hz,
42
43 CD₃OD @ 50 °C): δ_{ppm} 7.53 (d, $J = 7.6$ Hz, 1H), 7.25-7.10 (m, H-1, 5H), 7.05 (t, $J = 8.4$ Hz, 2H),
44
45 5.32 (s, 2H), 3.27 (t, $J = 5.2$ Hz, 4H), 3.04 (t, $J = 4.8$ Hz, 4H); ¹³C-NMR (101 Hz, MeOD @ 50
46
47 °C) δ_{ppm} 162.29 (d, $J = 244.9$ Hz, C-F), 157.7, 140.7, 134.7, 132.41 (d, $J = 3.0$ Hz), 128.10 (d, $J =$
48
49 8.1 Hz, 2C), 122.0, 121.7, 117.1, 115.23 (d, $J = 21.9$ Hz, 2C), 109.6, 50.4 (2C), 46.4 and 44.4 (2C);
50
51 LC-MS (APCI/ESI)⁺: m/z [M+H]⁺ = 311.2 (calculated for C₁₈H₁₉FN₄, 310.16).
52
53
54
55
56
57
58
59
60

1-(4-fluorobenzyl)-2-(4-(4-methoxyphenethyl)piperazin-1-yl)-1H-benzo[d]imidazole (3)

A solution of **2** (0.15 grams, 0.48 mmol), 1-(2-bromoethyl)-4-methoxybenzene (0.21 grams, 0.151 mL, 0.57 mmol) and triethyl amine (0.12 grams, 0.17 mL, 0.12 mmol) in toluene was refluxed (110 °C) for 48 h. After the completion of reaction, concentrated *in vacuo* and residue was dissolved in ethyl acetate (20 mL). This mixture was washed with sat. NaHCO₃ (2 × 15 mL), dried over sodium sulfate and concentrated *in vacuo*. Purification of residue by biotage flash chromatography at 5% MeOH: DCM and recrystallization from a mixture of pentane and DCM provided **3** as a white solid (0.12 grams, 50%); ¹H-NMR (400 Hz, CD₃OD @ 50 °C): δ_{ppm} 7.53 (d, *J* = 8.0 Hz, 1H), 7.23-7.12 (m, 6H), 7.13-7.09 (m, 1H), 7.08-7.03 (m, 2H), 6.84 (d, *J* = 8.8 Hz, 2H), 5.31 (s, 2H), 3.77 (s, 3H), 3.35-3.29 (m, 4H), 2.81-2.75 (m, 2H), 2.69 (m, 4H), 2.67-2.61 (m, 2H); ¹³C-NMR (101 Hz, MeOD @ 50 °C) δ_{ppm} 162.31 (d, *J* = 244.9 Hz, C-F), 158.3, 157.8, 140.8, 134.8, 132.46 (d, *J* = 2.7 Hz), 132.0, 129.2 (2C), 128.08 (d, *J* = 8.2 Hz, 2C), 121.9, 121.6, 117.0, 115.23 (d, *J* = 21.9, 2C), 113.6 (2C), 109.5, 60.2, 54.4, 52.4 (2C), 50.1 (2C), 46.5 and 31.8; LC-MS (APCI/ESI)⁺, found *m/z* = 445.2 [M+H]⁺ (calculated for C₂₇H₂₉FN₄O, 444.23); Purity = 99.9% (*t_r* = 4.035 min).

Synthesis of 4-N-Boc-((1H-benzo[d]imidazol-2-yl) amino) piperidine (5a). A mixture of 2-chlorobenzimidazole (**1a**) (2.0 grams, 13.2 mmol) and 4-amino-N-Boc-piperidine (3.15 grams, 15.7 mmol) in TEA (5.50 mL, 39.4 mmol) were stirred under a nitrogen atmosphere at 150 °C for 2 h. After the completion of reaction, dissolved in DCM (25 mL) followed by washing with NaHCO₃ (2 × 20 mL), brine (2 × 20 mL), dried over anhydrous Na₂SO₄ and concentrated *in vacuo*. Residue was washed with EtOAc to obtain **5a** as a white solid (2.49 grams, 60%). ¹H-NMR (300 MHz, DMSO-d₆) δ 10.59 (s, 1H), 7.12 (t, *J* = 6.9 Hz, 2H), 6.86 (dt, *J* = 12.4 and 7.2 Hz, 2H), 6.50 (d, *J* = 8.0 Hz, 1H), 3.90 (d, *J* = 13.3 Hz, 2H), 3.83 – 3.68 (m, 1H), 2.87 (d, *J* = 13.5 Hz, 2H), 1.93

(dd, $J = 12.6$ and 3.7 Hz, 2H), 1.41 (s, 9H), 1.39 – 1.27 (m, 2H). LC-MS (APCI/ESI)⁺, found $m/z = 317.1$ [M+H]⁺ (cal. for C₁₇H₂₄N₄O₂, 316.19).

Ethyl 4-((1-(4-fluorobenzyl)-1H-benzo[d]imidazol-2-yl)amino)piperidine-1-carboxylate (5b)

A neat mixture of **1b** (1.5 grams, 5.75 mmol) and ethyl 4-aminopiperidine-1-carboxylate (2.0 grams, 11.62 mmol) was heated to 170 °C and stirred for 4 h. After completion of the reaction, it was cooled to ambient temperature (23 °C), dissolved in DCM (50 mL), washed with saturated NaHCO₃ (2 × 20 mL), dried over sodium sulfate and concentrated *in vacuo*. Purification by column chromatography using 0.2-1% MeOH: DCM afforded **5b** as a white solid (2.3 grams, 98% yield); m.p. 175.8-178.7 °C; ¹H-NMR (400 Hz, CDCl₃): δ_{ppm} 7.55 (d, $J = 8.0$ Hz, 1H), 7.22-7.11 (m, H-1, 3H), 7.10-7.00 (m, 4H), 5.14 (s, 2H), 4.22-3.90 (m, 3H), 4.11 (q, $J = 8.0$ Hz, 2H), 4.24 (q, $J = 8.0$ Hz, 2H), 2.10 (m, 2H), 1.33 (m, 2H) and 1.25 (t, $J = 8.0$ Hz, 3H); LC-MS (APCI/ESI)⁺, found $m/z = 397.2$ [M+H]⁺ (calculated for C₂₂H₂₅FN₄O₂, 396.20).

N-(1-(4-methoxyphenethyl)piperidin-4-yl)-1H-benzo[d]imidazol-2-amine (5c)

A neat mixture of **1a** (0.1 grams, 0.657 mmol) and 1-(4-methoxyphenethyl)piperidin-4-amine (0.31 grams, 1.323 mmol) was heated to 170 °C and stirred for 4 h. After completion of the reaction, the reaction mixture was cooled down to ambient temperature (23 °C), dissolved in DCM (20 mL), washed with sat. NaHCO₃ (2 × 10 mL), dried over sodium sulfate and concentrated *in vacuo*. Purification by column chromatography using 0-1% MeOH: DCM afforded **5c** as a white solid (0.11 grams, 48% yield). ¹H-NMR (Methanol-*d*₄, 400 MHz) δ 7.24-7.17 (m, 2H), 7.13 (d, $J = 8.8$ Hz, 2H), 7.00-6.94 (m, 2H), 6.85 (d, $J = 8.4$ Hz, 2H), 3.76 (s, 3H), 3.72-3.62 (m, 1H), 3.10-2.96 (m, 2H), 2.82-2.71 (m, 2H), 2.64-2.54 (m, 2H), 2.29 (t, $J = 9.2$ Hz, 2H), 2.15-2.10 (m, 2H), 1.71-1.54 (m, 2H); ¹³C-NMR (101 MHz, MeOD) δ 158.7, 154.3, 137.6, 131.7, 129.2 (2C), 119.9,

1
2
3 113.6 (2C), 111.3 (4C), 60.3, 54.3, 52.0 (2C), 49.3, 32.0 and 31.7 (2C); LC-MS (APCI/ESI)⁺,
4 found $m/z = 351.2$ [M+H]⁺ (calculated for C₂₁H₂₆N₄O, 350.2), Purity = 97.1% ($t_r = 0.197$ min).
5
6
7
8
9
10
11
12
13

14
15 **4-((2-((1-(4-methoxyphenethyl)piperidin-4-yl)amino)-1H-benzo[d]imidazol-1-**
16 **yl)methyl)benzonitrile (5d)**
17
18

19
20 A solution of **1a** (0.3 grams, 1.967 mmol) and methyl iodide (1.5 grams, 10.709 mmol) in
21 DMF (3 mL) was charged with potassium carbonate (2.95 grams, 19.67 mmol). The resulting
22 reaction mixture was stirred at room temperature (23 °C) for 30 mins. After the completion of
23 reaction, quenched with water (10 mL), extracted with ethyl acetate (5 × 10 mL), dried over sodium
24 sulphate and concentrated to obtain the crude product (0.225 grams, 68% yield), which was washed
25 with *n*-pentane and used in next step without further purification.
26
27
28
29
30
31
32
33

34
35 A neat mixture of methylated product from previous step (0.075 grams, 0.450 mmol) and 1-(4-
36 methoxyphenethyl)piperidin-4-amine (0.2 grams, 0.90 mmol) was heated to 170 °C and stirred for
37 8 h. After the completion of the reaction, it was cooled to ambient temperature (23 °C), dissolved
38 in DCM (20 mL), washed with sat. NaHCO₃ (2 × 10 mL), dried over sodium sulfate and
39 concentrated *in vacuo*. Purification by column chromatography using 0-1% MeOH: DCM afforded
40 **5d** as a yellow solid (0.055 grams, 30% yield). ¹H-NMR (Methanol-*d*₄, 400 MHz) δ 7.33-7.27 (m,
41 1H), 7.21-7.11 (m, $J = 8.4$ Hz, 3H), 7.10-7.0 (m, 2H), 6.87 (d, $J = 8.0$ Hz, 2H), 3.88-3.80 (m, 1H),
42 3.76 (s, 3H), 3.55 (s, 3H), 3.21-3.11 (m, 2H), 2.87-2.76 (m, 2H), 2.74-2.65 (m, 2H), 2.39 (t, $J =$
43 9.2 Hz, 2H), 2.21-2.12 (m, 2H), 1.80-1.66 (m, 2H); ¹³C-NMR (101 MHz, MeOD) δ 158.4, 154.2,
44
45
46
47
48
49
50
51
52
53
54
55
56
57
58
59
60

1
2
3 141.2, 134.6, 131.4, 129.2 (2C), 120.7, 119.3, 114.4, 113.6 (2C), 107.0, 60.1, 54.3, 52.3 (2C), 49.7,
4
5 31.7, 31.2 (2C) and 27.2; LC-MS (APCI/ESI)⁺, found $m/z = 365.2$ [M+H]⁺ (calculated for
6
7 C₂₂H₂₈N₄O, 364.2), Purity = 95.5% ($t_r = 0.200$ min).
8
9

10 11 12 13 14 15 16 17 **4-((2-(piperidin-4-ylamino)-1H-benzo[d]imidazol-1-yl)methyl)benzotrile (6a).**

18
19 A mixture of **5a** (2.20 grams, 6.96 mmol), 4-(bromomethyl) benzonitrile (1.64 grams, 8.4 mmol) and
20
21 K₂CO₃ (2.40 grams, 17.4 mmol) in DMF (9 mL) was stirred under a nitrogen atmosphere at 70 °C
22
23 for 3 h. After the completion of the reaction, it was cooled to ambient temperature (23 °C) and
24
25 diluted with EtOAc (50 mL). The resulting mixture was washed with water (3 × 30 mL), 5% LiCl
26
27 (20 mL × 2) and brine (20 mL × 2), dried over sodium sulfate and concentrated *in vacuo*. The
28
29 residue was washed with diethyl ether and used in next step without further purification.
30
31
32

33
34 A suspension of *N*-Boc protected compound from the previous step in 4N HCl in dioxane (1 mL
35
36 per 0.100 grams) was stirred at ambient temperature (20 °C) for 2 h. After the completion of
37
38 reaction, dioxane was removed under vacuum and residue was taken in EtOAc (25 mL) and
39
40 neutralized with 15% NaOH (pH > 8) while stirring in an ice bath. The organic phase was dried
41
42 over anhydrous Na₂SO₄ and evaporated under vacuum to afford **6a** (2.50 grams, 5.80 mmol, 1 eq)
43
44 as a pale yellow solid (1.54 grams, 80% yield). ¹H-NMR (300 MHz, Methanol-*d*₄) δ 7.70 – 7.64
45
46 (m, 2H), 7.32 (dt, $J = 7.8, 0.9$ Hz, 1H), 7.28 – 7.22 (m, 2H), 7.05 (ddd, $J = 7.9, 6.9, 1.7$ Hz, 1H),
47
48 6.99 (ddd, $J = 7.9, 1.7, 0.7$ Hz, 1H), 6.94 (ddd, $J = 7.9, 6.9, 1.1$ Hz, 1H), 5.37 (s, 2H), 3.89 (tt, $J =$
49
50 11.1, 4.1 Hz, 1H), 3.07 (dt, $J = 12.9, 3.5$ Hz, 2H), 2.74 (td, $J = 12.5, 2.6$ Hz, 2H), 2.06 (dd, $J =$
51
52 12.7, 3.7 Hz, 2H), 1.46 (qd, $J = 11.9, 4.1$ Hz, 2H). ¹³C-NMR (101 MHz, Methanol-*d*₄) δ 153.95,
53
54
55
56
57
58
59
60

1
2
3 142.34, 141.70, 133.89, 132.25, 127.13, 121.29, 119.54, 118.05, 114.85, 111.02, 107.51, 50.16,
4
5 44.66, 44.23, 32.45. LC-MS (APCI/ESI): found $m/z = 331.9$ $[M+H]^+$ (cal. for $C_{20}H_{21}N_5$, 331.18).
6
7

8 **1-(4-fluorobenzyl)-N-(piperidin-4-yl)-1H-benzo[d]imidazol-2-amine (Nor-AST)**

9
10 A solution of **5b** (2.3 grams, 5.80 mmol) in HBr (48%, 17 mL) was refluxed (120 °C) for 3 h. After
11
12 completion of the reaction, it was cooled to 0 °C and treated with 2.5 M aqueous NaOH in dropwise
13
14 manner to neutralized excess of HBr (pH = 12-14). The extraction of organic compounds was done
15
16 with chloroform (5 × 20 mL). The combined organic layers were dried over sodium sulfate and
17
18 concentrated *in vacuo* to obtain Nor-AST as an orange solid (1.89 grams, 85% yield); ¹H-NMR
19
20 (400 Hz, CDCl₃): δ_{ppm} 7.52 (d, $J = 8.0$ Hz, 1H), 7.19-7.08 (m, 3H), 7.07-6.98 (m, 4H), 5.07 (s,
21
22 2H), 3.04 (dt, $J = 12.4$ and 4.8 Hz, 2H), 2.75 (td, $J = 12.0$ and 2.8 Hz, 2H), 2.41 (bs, 1H), 2.10 (m,
23
24 2H) and 1.32 (m, 2H); ¹³C-NMR (101 Hz, CDCl₃): δ_{ppm} 162.44 (d, $J = 247.3$ Hz, C-F), 153.3,
25
26 142.4, 134.5, 131.19 (d, $J = 3.3$ Hz), 128.22 (d, $J = 8.3$ Hz, 2C), 121.5, 119.8, 116.6, 116.13 (d, J
27
28 = 21.8 Hz, 2C), 107.2, 50.2, 45.2 (2C), 45.0 and 33.8 (2C); LC-MS (APCI/ESI)⁺, found $m/z =$
29
30 325.2 $[M+H]^+$ (calculated for $C_{19}H_{21}FN_4$, 324.18), Purity = 95.2% ($t_r = 2.819$ min).
31
32
33
34
35
36

37 **General procedure 1 for the synthesis of AST and compounds 7-16:** A solution of 2-chloro-
38
39 1H-benzo[d]imidazole (1 equivalent) in acetone was charged with K₂CO₃ (2.5 equivalent) and
40
41 respective benzyl bromide (1.5 equivalent). The resulting reaction mixture was stirred at room
42
43 temperature (23 °C) for 4-6 hours. After completion of the reaction, it was filtered and
44
45 concentrated. The crude product was washed with *n*-pentane to obtain **4** and used in next step
46
47 without further purification.
48
49

50
51
52 A mixture of respective benzylated benzimidazole intermediate **4** (1 equivalents) and 1-(4-
53
54 methoxyphenethyl)piperidin-4-amine (2 equivalents) was heated to 170 °C and stirred for 6-12 h.
55
56
57

1
2
3 After the completion of reaction, cooled to ambient temperature (23 °C) and resulting solid was
4 dissolved in DCM, washed with saturated solution of sodium bicarbonate (twice), water (twice)
5 and brine. The organic phase was dried over sodium sulphate and concentrated *in vacuo* to obtain
6 crude product, which was purified by column chromatography using 1-10% MeOH: DCM to
7 afford pure compounds.
8
9

10
11
12
13
14
15
16 **1-(4-fluorobenzyl)-N-(1-(4-methoxyphenethyl)piperidin-4-yl)-1H-benzo[d]imidazol-2-amine**
17
18 **(AST)**

19
20 White solid (72% yield); ¹H-NMR (400 Hz, CD₃OD): δ_{ppm} 7.32 (d, *J* = 8.0 Hz, 1H), 7.19-7.10 (m,
21 4H), 7.08-7.00 (m, 4H), 6.95 (td, *J* = 8.0 and 0.8 Hz, 1H) 6.84 (dd, *J* = 8.8 and 2.4 Hz, 2H), 5.25
22 (s, 2H), 3.84 (tt, *J* = 12.0 and 4.0 Hz, 1H), 3.76 (s, 3H), 3.01 (m, 2H), 2.76 (m, 2), 2.58 (m, 2H),
23 2.27 (m, 2H), 2.09 (m, 2H), 1.69-1.53 (m, 2H); ¹³C-NMR (101 Hz, CD₃OD): δ 162.19 (d, *J* =
24 242.4 Hz), 158.2, 154.0, 141.7, 134.0, 132.4 (d, *J* = 2.02 Hz) , 131.8, 129.2 (2C), 128.23 (d, *J* =
25 8.1 Hz; 2C), 121.1, 119.4, 115.06 (d, *J* = 21.8 Hz, 2C), 114.7, 113.6 (2C), 107.7, 60.4, 54.3, 52.2,
26 49.9, 43.9, 32.0 and 31.5; LC-MS (APCI/ESI)⁺, found *m/z* = 459.2 [M+H]⁺ (calculated for
27 C₂₈H₃₁FN₄O, 458.25); Purity = 95.7%, (*t_r* = 3.525 min).
28
29
30
31
32
33
34
35
36
37
38

39
40 **1-(3-fluorobenzyl)-N-(1-(4-methoxyphenethyl)piperidin-4-yl)-1H-benzo[d]imidazol-2-amine**
41
42 **(7)**

43
44 White solid (70%); ¹H-NMR (Methanol-*d*₄, 400 MHz) δ 7.37-7.28 (m, 2H), 7.18-7.12 (d, *J* = 8.8
45 Hz, 2H), 7.09-7.01 (m, 2H), 7.0-6.91 (m, 2H), 6.98-6.80 (m, 2H), 5.31 (s, 2H), 3.86 (tt, *J* = 12.0
46 and 4.0 Hz, 1H), 3.77 (s, 3H), 3.10-2.95 (m, 2H), 2.83-2.70 (m, 2H), 2.66-2.52 (m, 2H), 2.29 (td,
47 *J* = 9.2 and 2.0 Hz, 2H), 2.15-2.05 (m, 2H), 1.72-1.59 (m, 2H); ¹³C-NMR (101 MHz, MeOD) δ
48 163.09 (d, *J* = 245.3 Hz, C-F), 158.2, 154.0, 141.6, 139.45 (d, *J* = 6.98 Hz), 134.0, 131.8, 130.25
49 (d, *J* = 8.27 Hz), 129.2 (2C), 122.0, 121.1, 119.5, 114.7, 113.89 (d, *J* = 21.3 Hz), 113.6 (2C), 113.07
50
51
52
53
54
55
56
57
58
59
60

(d, $J = 22.6$ Hz), 107.6, 60.4, 54.3, 52.3 (2C), 49.9, 44.0, 31.9, 31.3 (2C); LC-MS (APCI/ESI)⁺, found $m/z = 459.1$ [M+H]⁺ (calculated for C₂₈H₃₁FN₄O, 458.25); Purity = 97.8%, ($t_r = 3.989$ min).

1-(2-fluorobenzyl)-N-(1-(4-methoxyphenethyl)piperidin-4-yl)-1H-benzo[d]imidazol-2-amine (8)

White solid (64%); ¹H-NMR (Methanol-*d*₄, 400 MHz) δ 7.35-7.32 (m, 1H), 7.31-7.36 (m, 1H), 7.18-7.11 (m, 3H), 7.09-7.00 (m, 3H), 6.95 (ddd, $J = 8.4, 7.2$ and 1.2 Hz), 6.89-6.81 (m, 3H), 5.34 (s, 2H), 3.86 (tt, $J = 12.0$ and 4.0 Hz, 1H), 3.78 (s, 3H), 3.09-3.0 (m, 2H), 2.83-2.71 (m, 2H), 2.64-2.54 (m, 2H), 2.30 (td, $J = 12$ and 3.6 Hz, 2H), 2.16-2.05 (m, 2H), 1.69-1.53 (m, 2H); ¹³C-NMR (101 MHz, MeOD) δ 160.56 (d, $J = 245.2$ Hz, C-F), 158.2, 154.1, 141.7, 133.9, 131.9, 129.2 (2C), 128.8, 127.9 (d, $J = 3.7$ Hz), 124.2, 123.34 (d, $J = 14.7$ Hz), 121.1, 119.4, 115.03 (d, $J = 21.2$ Hz), 114.9, 114.7, 113.6 (2C), 107.5, 60.4, 54.3, 52.2 (2C), 50.0, 39.0, 31.9 and 31.2 (2C); LC-MS (APCI/ESI)⁺, found $m/z = 459.1$ [M+H]⁺ (calculated for C₂₈H₃₁FN₄O, 458.25); Purity = 99.2%, ($t_r = 3.886$ min).

4-((2-((1-(4-methoxyphenethyl)piperidin-4-yl)amino)-1H-benzo[d]imidazol-1-yl)methyl)benzotrile (9)

Pink solid (40%); ¹H-NMR (Methanol-*d*₄, 400 MHz) δ 7.69 (d, $J = 8.4$ Hz, 2H), 7.36 (d, $J = 8.0$ Hz, 1H), 7.27 (d, $J = 8.4$ Hz, 2H), 7.15 (d, $J = 8.4$ Hz, 2H), 7.08 (t, $J = 7.4$ Hz, 1H), 7.05 - 7.0 (m, 1H), 7.0 - 6.95 (m, 1H), 6.86 (d, $J = 8.4$ Hz, 2H), 5.40 (s, 2H), 3.94-3.83 (m, 1H), 3.77 (s, 3H), 3.22-3.07 (m, 2H), 2.88-2.77 (m, 2H), 2.77-2.66 (m, 2H), 2.45 (t, $J = 12.4$ Hz, 2H), 2.21-2.10 (m, 2H), 1.78-1.61 (m, 2H); ¹³C-NMR (101 MHz, MeOD) δ 158.4, 153.9, 142.3, 141.6, 132.3 (2C), 131.1, 129.2 (3C), 127.1 (2C), 121.4, 119.7, 118.0, 114.9, 113.7 (2C), 111.0, 107.6, 59.9, 54.3,

52.0 (2C), 49.7, 44.3, 31.4, and 31.0 (2C); LC-MS (APCI/ESI)⁺, found $m/z = 466.2$. [M+H]⁺
(calculated for C₂₉H₃₁N₅O, 465.25); Purity = 99.9%, ($t_r = 1.974$ min).

3-((2-((1-(4-methoxyphenethyl)piperidin-4-yl)amino)-1H-benzo[d]imidazol-1-yl)methyl)benzotrile (10)

White solid (15%); ¹H-NMR (Methanol-*d*₄, 400 MHz) δ 7.68-7.67 (m, 1H), 7.55-7.45 (m, 2H), 7.43-7.33 (m, 2H), 7.14 (d, $J = 7.8$ Hz, 2H), 7.11-7.01 (m, 2H), 7.03-6.95 (m, 1H), 6.85 (d, $J = 8.0$ Hz, 2H), 5.35 (s, 2H), 3.98-3.83 (m, 1H), 3.77 (s, 3H), 3.20-3.07 (m, 2H), 2.87-2.77 (m, 2H), 2.76-2.66 (m, 2H), 2.43 (t, $J = 12.0$ Hz, 2H), 2.21-2.09 (m, 2H), 1.80-1.60 (m, 2H); ¹³C-NMR (101 MHz, MeOD) δ 158.4, 154.0, 141.7, 138.4, 133.9, 131.6, 131.0 (2C), 129.9, 129.6, 129.2 (2C), 127.4, 119.7, 118.0, 115.0, 113.8 (2C), 112.6, 107.6, 59.9, 54.3, 52.1 (2C), 49.8, 44.0, 31.7, and 31.2 (2C); LC-MS (APCI/ESI)⁺, found $m/z = 466.2$. [M+H]⁺ (calculated for C₂₉H₃₁N₅O, 465.25); Purity = 98.9%, ($t_r = 1.977$ min).

2-((2-((1-(4-methoxyphenethyl)piperidin-4-yl)amino)-1H-benzo[d]imidazol-1-yl)methyl)benzotrile (11)

White solid (30%); ¹H-NMR (Methanol-*d*₄, 400 MHz) δ 7.80 (dd, $J = 6.8$ and 0.96 Hz, 1H), 7.52 (td, $J = 7.60$ and 1.2 Hz, 1H), 7.44 (td, $J = 7.60$ and 0.8 Hz, 1H), 7.36 (d, $J = 7.60$ Hz, 1H), 7.14 (d, $J = 8.4$ Hz, 2H), 7.08 (ddd, $J = 8.4$, 6.0 and 2.4 Hz, 1H), 6.98-6.90 (m, 2H), 6.88-6.77 (m, $J = 8.4$ Hz, 3H), 5.52 (s, 2H), 3.95-3.82 (m, 1H), 3.77 (s, 3H), 3.14-3.02 (m, 2H), 2.81-2.74 (m, 2H), 2.68-2.59 (m, 2H), 2.34 (t, $J = 12.0$ Hz, 2H), 2.19-2.09 (m, 2H), 1.75-1.61 (m, 2H); ¹³C-NMR (101 MHz, MeOD) δ 158.3, 154.1, 141.7, 141.0, 133.9, 131.6, 131.1, 131.5, 129.2 (2C), 127.9, 126.2, 121.4, 119.6, 116.2, 114.9, 113.6 (2C), 110.7, 107.5, 60.2, 54.3, 52.2 (2C), 49.9, 43.3, 31.8, and

1
2
3 31.3 (2C); LC-MS (APCI/ESI)⁺, found $m/z = 466.2$. $[M+H]^+$ (calculated for C₂₉H₃₁N₅O, 465.25);
4
5 Purity = 99.01% ($t_r = 2.027$ min).
6
7
8
9
10

11
12 **4-((2-((1-(4-methoxyphenethyl)piperidin-4-yl)amino)-1H-benzo[d]imidazol-1-**
13
14 **yl)methyl)benzoic acid (12)**
15

16 White solid (15%); ¹H-NMR (DMSO-*d*₆, 400 MHz @ 80 °C) δ 10.74 (s, 1H), 8.04 (s, 1H), 7.82
17
18 (d, $J = 8.2$ Hz), 7.38 (d, $J = 8.3$ Hz), 7.16 (d, $J = 8.6$ Hz, 2H), 7.03-6.91 (m, 4H), 6.87 (d, $J = 8.6$
19
20 Hz, 2H), 5.04 (s, 2H), 3.97-3.82 (m, 1H), 3.06-2.92 (m, 2H; overlapping with DMSO water peak),
21
22 2.89-2.72 (m, 6H), 1.96-1.86 (m, 2H), 1.81-1.65 (m, 2H); ¹³C-NMR (101 MHz, DMSO-*d*₆) ¹³C
23
24 NMR (101 MHz, DMSO) δ 166.1, 158.3, 154.8, 140.7, 134.3, 130.5, 130.3, 130.1 (2C), 128.8,
25
26 128.1 (2C), 127.6 (2C), 121.6, 121.0, 114.3 (2C), 109.4, 108.5, 55.5 (2C), 51.9 (2C), 50.5, 49.9,
27
28 49.6 and 43.33 (2C); LC-MS (APCI/ESI)⁺, found $m/z = 485.2$ $[M+H]^+$ (calculated for C₂₉H₃₂N₄O₃,
29
30 458.25); Purity = 97.0%, ($t_r = 3.989$ min).
31
32
33
34
35

36 **4-((2-((1-(4-methoxyphenethyl)piperidin-4-yl)amino)-1H-benzo[d]imidazol-1-**
37
38 **yl)methyl)benzamide (13)**
39

40 White solid (29%); ¹H-NMR (Methanol-*d*₄, 400 MHz) δ 7.82 (d, $J = 8.4$ Hz, 2H), 7.35 (d, $J = 7.8$
41
42 Hz, 1H), 7.20 (d, $J = 6.8$ Hz, 2H), 7.13 (d, $J = 8.6$ Hz, 2H), 7.11-7.01(m, 2H), 6.99-6.91 (m, 1H),
43
44 6.85 (d, $J = 8.4$ Hz, 2H), 5.37 (s, 2H), 3.90-3.80 (m, 1H), 3.77 (s, 3H), 3.08-2.94 (m, 2H), 2.81-
45
46 2.71 (m, 2H), 2.63-2.53 (m, 2H), 2.28 (t, $J = 12.0$ Hz, 2H), 2.14-2.04 (m, 2H), 1.72-1.56 (m, 2H);
47
48 ¹³C-NMR (101 MHz, MeOD) δ 170.4, 158.2, 154.1, 141.7, 140.6, 134.0, 132.9, 131.8, 129.2 (2C),
49
50 127.7 (2C), 126.3 (2C), 121.1, 119.4, 114.7, 113.6 (2C), 107.6, 60.4, 54.2, 52.2 (2C), 49.9, 44.3,
51
52
53
54
55
56
57
58
59
60

1
2
3 31.9, and 31.4 (2C); LC-MS (APCI/ESI)⁺, found $m/z = 483.9$ [M+H]⁺ (calculated for C₂₉H₃₃N₅O₂,
4 483.9); Purity = 95.81% ($t_r = 2.264$ min).
5
6
7
8
9
10

11 **N-(1-(4-methoxyphenethyl)piperidin-4-yl)-1-(4-(methylsulfonyl)benzyl)-1H-**
12 **benzo[d]imidazol-2-amine (14)**
13
14
15

16 White solid (38%); ¹H-NMR (Methanol-*d*₄, 400 MHz) δ 7.88 (d, *J* = 8.4 Hz, 2H), 7.42-7.31 (m,
17 3H), 7.13 (d, *J* = 8.6 Hz, 2H), 7.07 (td, *J* = 6.9 and 1.2 Hz, 1H), 7.03-6.99 (m, 1H), 6.99-6.91 (m,
18 1H), 6.85 (d, *J* = 8.4 Hz, 2H), 5.37 (s, 2H), 3.90-3.80 (m, 1H), 3.77 (s, 3H), 3.06 (s, 3H), 3.04-2.94
19 (m, 2H), 2.81-2.71 (m, 2H), 2.63-2.53 (m, 2H), 2.28 (t, *J* = 12.0 Hz, 2H), 2.14-2.04 (m, 2H), 1.72-
20 1.56 (m, 2H); ¹³C-NMR (101 MHz, MeOD) δ ¹³C-NMR (101 MHz, MeOD) δ 158.3, 154.1, 143.0,
21 141.8, 140.1, 134.0, 132.0, 129.2 (2C), 127.4, 127.3 (2C), 121.3, 119.6, 115.0, 113.7 (2C), 107.6,
22 102.1, 60.1, 54.4, 52.1 (2C), 50.0, 44.3, 43.0, 31.9, 31.4 (2C); LC-MS (APCI/ESI)⁺, found $m/z =$
23 519.2 [M+H]⁺ (calculated for C₂₉H₃₄N₄O₃, 518.68); Purity = 98.49% ($t_r = 1.991$ min).
24
25
26
27
28
29
30
31
32
33
34

35 **1-(4-((1-(4-methoxyphenethyl)piperidin-4-yl)amino)-1H-benzo[d]imidazol-1-**
36 **yl)methyl)phenyl)ethan-1-one (15)**
37
38
39

40 White solid (30%); ¹H-NMR (Methanol-*d*₄, 400 MHz) δ 7.92 (d, *J* = 8.0 Hz, 2H), 7.35 (d, *J* = 8.0
41 Hz, 1H), 7.22 (d, *J* = 8.4 Hz, 2H), 7.13 (d, *J* = 8.6 Hz, 2H), 7.07(td, *J* = 8 and 1.2 Hz, 1H), 7.03-
42 6.99 (m, 1H), 6.99-6.92 (m, 1H), 6.84 (d, *J* = 8.4 Hz, 2H), 5.36 (s, 2H), 3.92-3.82 (m, 1H), 3.76
43 (s, 3H), 3.15-2.99 (m, 2H), 2.81-2.71 (2H, m), 2.68-2.58 (m, 2H), 2.37 (t, *J* = 12.0 Hz, 2H), 2.19-
44 2.07 (m, 2H), 1.77-1.60 (m, 2H); ¹³C-NMR (101 MHz, MeOD) δ 198.5, 158.3, 154.0, 142.1, 141.6,
45 136.2, 134.0, 131.4, 129.2 (2C), 128.5 (2C), 126.5 (2C), 121.2, 119.5, 114.8, 113.6 (2C), 107.7,
46
47
48
49
50
51
52
53
54
55
56
57
58
59
60

60.1, 54.3, 52.1 (2C), 49.7, 44.4, 31.6, 31.1 (2C) and 25.3; LC-MS (APCI/ESI)⁺, found m/z = 483.2 [M+H]⁺ (calculated for C₃₀H₃₄N₄O₂, 482.27); Purity = 95.54% (t_r = 2.147 min).

N-(1-(4-methoxyphenethyl)piperidin-4-yl)-1-(pyridin-3-ylmethyl)-1H-benzo[d]imidazol-2-amine (16)

Yellow solid (36%); ¹H-NMR (Methanol-*d*₄, 400 MHz) δ 8.47 (d, *J* = 8.4 Hz, 2H), 7.36 (d, *J* = 7.60 Hz, 1H), 7.17-7.11 (m, 4H), 7.11-7.06 (m, 1H), 7.05-6.99 (m, 2H), 6.86 (d, *J* = 8.4 Hz, 2H), 5.39 (s, 2H), 3.93-3.81 (m, 1H), 3.78 (s, 3H), 3.11-3.03 (m, 2H), 2.84-2.72 (m, 2H), 2.66-2.56 (m, 2H), 2.32 (t, *J* = 12.0 Hz, 2H), 2.15-2.08 (m, 2H), 1.72-1.60 (m, 2H); ¹³C-NMR (101 MHz, MeOD) δ 158.4, 153.9, 149.0 (2C), 147.2, 141.5, 133.9, 130.8, 129.2 (2C), 121.8, 121.4, 119.7, 116.4, 114.9, 113.7 (2C), 107.5, 59.7, 54.3, 52.0 (2C), 49.4, 43.6, 31.3 (2C) and 30.8; LC-MS (APCI/ESI)⁺, found m/z = 442.2. [M+H]⁺ (calculated for C₂₇H₃₁N₅O, 441.25); Purity = 96.1% (t_r = 1.916 min).

General procedure 2 for the synthesis of 17-20: A solution of *Nor*-AST (1 equivalent) and respective phenylethylbromide (1.3 equivalents) in acetonitrile was charged with K₂CO₃ (2.5 equivalents). The resulting reaction mixture was refluxed for 5-24 hours. After completion of the reaction, it was filtered and concentrated *in vacuo*. The residue was dissolved in DCM and washed with NaHCO₃ (2 ×) and brine (2 ×), dried over anhydrous sodium sulphate and concentrated *in vacuo*. The crude product was purified by column chromatography using 0 – 10% MeOH/DCM.

4-((2-((1-(4-hydroxyphenethyl)piperidin-4-yl)amino)-1-benzimidazol-2-yl)methyl)benzonitrile (17)

Yellow solid (63%); ¹H-NMR (600 MHz, Methanol-*d*₄) δ 7.67 (d, *J* = 8.5 Hz, 2H), 7.35 (dt, *J* = 7.9, 0.9 Hz, 2H), 7.26 (d, *J* = 8.7 Hz, 2H), 7.08 (d, *J* = 8.5 Hz, 3H), 7.04 – 7.02 (m, 1H), 6.98 (ddd,

1
2
3 $J = 8.1, 7.3, 1.1$ Hz, 1H), 6.75 (d, $J = 8.6$ Hz, 2H), 5.41 (s, 2H), 3.96 (tt, $J = 10.7, 4.0$ Hz, 1H),
4
5 3.38 (m, 2H), 3.01 (m, 2H), 2.90 – 2.81 (m, 4H), 2.24 (m, 2H), 1.81 (m, 2H); ^{13}C NMR (151 MHz,
6
7 MeOD) δ 155.9, 153.7, 142.2, 141.3, 133.8, 132.3 (2C), 129.3 (2C), 128.6, 127.1 (2C), 121.4, 119.8, 118.0,
8
9 115.1 (2C), 114.9, 111.0, 107.7, 59.2, 51.8 (2C), 48.8, 44.3, 30.7 and 30.2 (2C); LC-MS (APCI/ESI):
10
11 found $m/z = 452.1$ $[\text{M}+\text{H}]^+$ (cal. for $\text{C}_{28}\text{H}_{29}\text{N}_5\text{O}$, 451.24); Purity: 98% ($t_{\text{R}} = 0.587$ min)

12
13
14
15 **1-(4-fluorobenzyl)-N-(1-(3-methoxyphenethyl)piperidin-4-yl)-1H-benzo[d]imidazol-2-amine**
16
17
18 **(18)**

19
20 White solid (78%); ^1H -NMR (600 MHz, Methanol- d_4) δ 7.35 – 7.33 (d, $J = 7.74$ Hz, 1H), 7.20 (td,
21
22 $J = 1.7, 7.8$ Hz, 1H), 7.18 – 7.13 (m, 3H), 7.08 – 7.00 (m, 4H), 6.96 (td, $J = 8.1$ and 1.1, Hz, 1H),
23
24 6.93 (dd, $J = 8.2$ and 1.0, Hz, 1H), 6.88 (td, $J = 7.4$ and 1.1 Hz, 1H), 5.26 (s, 2H), 3.88 (t, $J = 10.9$
25
26 Hz, 1H), 3.84 (s, 3H), 3.10 (d, $J = 11.7$ Hz, 2H), 2.94 – 2.77 (m, 2H), 2.76 – 2.63 (m, 2H), 2.40
27
28 (td, $J = 12.2$ Hz, 2H), 2.20 – 2.03 (m, 2H), and 1.77 – 1.58 (m, 2H); ^{13}C -NMR (151 MHz, MeOD)
29
30 δ 162.20 (d, $J = 244.58$ Hz, C-F), 157.5, 153.9, 141.6, 134.0, 132.4 (d, $J = 3.54$ Hz), 129.9, 128.23
31
32 (d, $J = 7.7$ Hz, 2C), 127.5, 127.4, 121.1, 120.3, 119.5, 115.06 (d, $J = 22$ Hz, 2C), 114.7, 110.2,
33
34 107.7, 58.2, 54.4, 52.0 (2C), 49.7, 43.9, 31.1 (2C) and 27.2; LC-MS (APCI/ESI) $^+$, found $m/z =$
35
36 458.9 $[\text{M}+\text{H}]^+$ (calculated for $\text{C}_{28}\text{H}_{31}\text{FN}_4\text{O}$, 458.58); Purity = 99.16% ($t_{\text{R}} = 2.487$ min).

37
38
39
40
41 **1-(4-fluorobenzyl)-N-(1-(2-methoxyphenethyl)piperidin-4-yl)-1H-benzo[d]imidazol-2-amine**
42
43
44 **(19)**

45
46 White solid (71%); ^1H -NMR (600 MHz, Methanol- d_4) δ 7.34 (d, $J = 7.8$ Hz, 1H), 7.20 (t, $J = 8.0$
47
48 Hz, 1H), 7.15 (m, 2H), 7.08 – 6.99 (m, 4H), 6.98-6-39 (m, 2H), 6.82 – 6.79 (m, 2H), 6.77 (dd, $J =$
49
50 2.4, 8.2 Hz, 1H), 5.25 (s, 2H), 3.86 (tt, $J = 4.2, 10.8$ Hz, 1H), 3.09-3.00 (m, 2H), 2.85-2.78 (m,
51
52 2H), 2.74 – 2.61 (m, 2H), 2.35 (t, $J = 11.8$ Hz, 2H), 2.18 – 2.07 (m, 2H), 1.67 (m, 2H); ^{13}C -NMR
53
54 (151 MHz, MeOD) δ 162.20 (d, $J = 244.58$ Hz), 159.9, 153.9, 141.6, 141.2, 134.0, 132.4 (d, $J =$
55
56

2.66 Hz), 129.1, 128.23 (d, $J = 8.1$ Hz, 2C), 128.2, 121.1, 120.6, 119.5, 115.07 (d, $J = 22$ Hz, 2C), 114.7, 114.0, 111.3, 107.7, 59.8, 54.2, 52.1 (2C), 49.7, 43.9, 32.7 and 31.3 (2C); LC-MS (APCI/ESI)⁺, found $m/z = 458.9$ [M+H]⁺ (calculated for C₂₈H₃₁FN₄O, 458.58); Purity = 99.50% ($t_r = 2.469$ min).

1-(4-fluorobenzyl)-N-(1-phenethylpiperidin-4-yl)-1H-benzo[d]imidazol-2-amine (20)

White solid (79%); ¹H-NMR (600 MHz, Methanol-*d*₄) δ 7.34 (d, $J = 7.8$ Hz, 1H), 7.29 (t, $J = 7.5$ Hz, 1H), 7.25 – 7.17 (m, 3H), 7.17-7.12 (m, 2H), 7.08 – 6.99 (m, 4H), 6.96 (t, $J = 7.6$ Hz, 1H), 5.25 (s, 2H), 3.96 – 3.81 (m, 1H), 3.19 – 2.99 (m, 2H), 2.97 – 2.77 (m, 2H), 2.77 – 2.63 (m, 2H), 2.38 (t, $J = 11.9$ Hz, 2H), 2.13 (d, $J = 13.0$ Hz, 2H) and 1.69 (m, 2H); ¹³C-NMR (151 MHz, MeOD) δ 163.0 and 161.4 (d, $J = 244.58$ Hz, C-F), 153.9, 141.5, 139.5, 134.0 (d, $J = 2.3$ Hz, 2C), 132.39 (d, $J = 2.31$ Hz), 128.3 (m, 3C), 128.2 (2C), 128.0, 125.9, 121.1, 119.5, 115.07 (d, $J = 21.8$ Hz), 114.7, 107.7, 59.9, 52.1 (2C), 49.7, 43.9, 32.6, 31.2 (2C); LC-MS (APCI/ESI)⁺, found $m/z = 428.9$ [M+H]⁺ (calculated for C₂₇H₂₉FN₄, 428.24); Purity = 99.57% ($t_r = 2.452$ min).

4-(2-(4-((1-(4-fluorobenzyl)-1H-benzo[d]imidazol-2-yl)amino)piperidin-1-yl)ethyl)phenol (DM-AST)

A solution of AST (0.1 grams, 0.02 mmol) in HBr (48%, 5 mL) was refluxed (120 °C) for 6 h. After completion of reaction, the reaction mixture was cooled to 0 °C and treated with 1 M aqueous NaOH in dropwise manner to neutralized excess of HBr (pH = 12-14). The organic components were extracted with 10% methanol in DCM (5 × 10 mL), and combined organic layers was dried over sodium sulfate. The removal of solvent under reduced pressure furnished DM-AST as an orange solid (0.4 grams, 45% yield); ¹H-NMR (400 Hz, DMSO): δ_{ppm} 9.20 { bs, 1H, OH (disappears in D₂O shake)}, 7.24 (m, 3H), 7.15 (d, $J = 8.0$ Hz, 2H), 7.06 (d, $J = 8.0$ Hz, 1H), 7.02 (d, $J = 8.4$ Hz, 2H), 6.94 (t, $J = 8.0$ Hz, 1H), 6.84 (t, $J = 7.6$ Hz, 1H), 6.68 (d, $J = 8.0$ Hz, 2H), 6.50

1
2
3 (bs, 1H), 5.27 (s, 2H), 3.85 (m, 1H), 3.05 (m, 2H), 2.77-2.66 (m, 4H), 2.37 (m, 2H), 2.04 (m, 2H),
4
5 1.79-1.62 (m, 2H); ^{13}C -NMR (101 Hz, DMSO): 167.6, 161.90 (d, $J = 243.0$ Hz, C-F), 154.4, 143.3,
6
7 142.8, 134.8, 133.81 (d, $J = 2.41$ Hz), 129.9 (2C), 129.42 (d, $J = 8.2$ Hz, 2C), 121.0, 119.0, 115.74
8
9 (overlapping d, $J = 18.9$ Hz, 2C), 115.7 (3C), 108.3, 59.8, 52.3 (2C), 50.0, 44.4 (2C), 32.0 and
10
11 31.6; LC-MS (APCI/ESI) $^+$, found $m/z = 445.2$ [M+H] $^+$ (calculated for $\text{C}_{27}\text{H}_{29}\text{FN}_4\text{O}$, 444.23);
12
13 Purity = 95.2%, ($t_r = 2.635$ min).
14
15
16
17

18 **Material and method of *in vitro* Antiplasmodium assay:**

19 **(a) Parasite lactate dehydrogenase assay at UCT for *in Vitro* Antiplasmodium Activity**

20
21 **Testing:** All parasite strains were acquired from MR4 (Malaria Research and Reference reagent
22
23 Resource Centre, Manassas, VA). Briefly, the respective stock solutions of CQ diphosphate and
24
25 test compounds were prepared to 2 mg/mL in distilled water (for CQ) and 100% DMSO (for test
26
27 compounds) then stored at -20 °C and further dilutions prepared on the day of the experiment.
28
29 Synchronized trophozoite-stage cultures of *Pf*NF54 (CQS) and *Pf*K1 (CQR) were prepared to 2%
30
31 parasitemia and 2% haematocrit. Compounds were tested at starting concentrations of 10 000
32
33 ng/mL (1 000 ng/mL for CQ), which were then serially diluted 2-fold in complete medium to give
34
35 10 concentrations with a final volume of 200 μL in each well. Parasites were incubated in the
36
37 presence of the compounds at 37 °C and under normal hypoxic conditions for 48 h. Following
38
39 incubation, 100 μL of MalStat reagent and 15 μL of re-suspended culture were combined, followed
40
41 by addition of 25 μL of NBT (nitro blue tetrazolium chloride). The plates were kept in the dark for
42
43 about 10 min to fully develop and absorbance measured at 620 nm on a microplate reader. Raw
44
45 data were exported to Microsoft Excel for dose-response analysis.
46
47
48
49
50
51
52

53 **(b) Modified [^3H]-hypoxanthine incorporation assay at Swiss TPH for *in vitro* antiplasmodium**
54
55 **activity testing:** Compounds were screened against multidrug resistant (*Pf*K1) and sensitive
56
57
58
59
60

1
2
3 (*Pf*NF54) strains of *P. falciparum* in vitro using the modified [³H]-hypoxanthine incorporation
4 assay.¹⁷ Plasmodium falciparum was cultivated in a variation of the medium previously
5 described,^{18,19} consisting of RPMI 1640 supplemented with 0.5% ALBUMAX® II, 25 mM HEPES,
6 25 mM NaHCO₃ (pH 7.3), 0.36mM hypoxanthine, and 100 microgram/ml neomycin. Human
7 erythrocytes served as host cells. Cultures were maintained at 37 °C in an atmosphere of 3% O₂,
8 4% CO₂, and 93% N₂ in humidified modular chambers. Compounds were dissolved by sonication
9 in DMSO (10mg/ml) and diluted in hypoxanthine-free culture medium. Infected erythrocytes (100
10 microliter per well with 2.5% haematocrit and 0.3% parasitemia) were added to each drug titrated
11 in 100 microliter duplicates over a 64-fold range. After 48 h incubation, 0.5 microCi of [³H]
12 hypoxanthine in 50 microliter media was added and plates were incubated for an additional 24 h.
13 Parasites were harvested onto glass-fibre filters and radioactivity was counted using a Beta plate
14 liquid scintillation counter (Wallac, Zurich). The results were recorded as counts per minute (cpm)
15 per well at each drug concentration and expressed as a percentage of the untreated controls. Fifty
16 percent inhibitory concentrations (IC₅₀) were estimated by linear interpolation.²⁰
17
18
19
20
21
22
23
24
25
26
27
28
29
30
31
32
33
34
35

36 ***In Vitro* Gametocyte Activity Testing:** Gametocytes were produced as per method reported by
37 Reader and co-workers.²¹ Late stage gametocytocidal dual point screens and IC₅₀ determination
38 were cross-validated on the luciferase reporter and ATP bioluminescence platforms.²¹ All assays
39 were performed in parallel using the same stock compounds, diluted fresh with complete culture
40 medium from 10 mM stock solutions in DMSO (0.5% v/v), and included methylene blue as drug
41 control. IC₅₀s were generated with GraphPad Prism 6, for n=3 independent biological replicates
42 performed in technical triplicates, ± S.E.
43
44
45
46
47
48
49
50
51
52
53
54
55
56
57
58
59
60

1
2
3 ***In Vitro P. berghei* Liver Stage Assay:** Inhibition of liver stage infection by test compounds was
4 assessed by measuring the luminescence intensity in Huh-7 cells infected with a firefly luciferase-
5 expressing *P. berghei* ANKA parasite line, as previously described.¹³
6
7

8
9
10 **Assay procedure:** Briefly, Huh-7 cells, a human hepatoma cell line, were cultured in 1640 RPMI
11 medium supplemented with 10% v/v fetal bovine serum, 1% v/v nonessential amino acids, 1% v/v
12 penicillin/streptomycin, 1% v/v glutamine, and 10 mM 4-(2-hydroxyethyl)-1-
13 piperazineethanesulfonic acid (HEPES), pH 7, and maintained at 37 °C with 5% CO₂. For infection
14 assays, Huh-7 cells (1.0 × 10⁴ per well) were seeded in 96-well plates the day before drug treatment
15 and infection. The medium was replaced by infection medium (*i.e.* culture medium supplemented
16 with gentamicin (50 µg/mL) and amphotericin B (0.8 µg/mL)) containing the appropriate
17 concentration of each compound approximately 1 h prior to infection with sporozoites freshly
18 obtained through disruption of salivary glands of infected female *Anopheles stephensi* mosquitoes.
19 An amount of the DMSO solvent equivalent to that present in the highest compound concentration
20 was diluted in infection medium and used as control. Sporozoite addition was followed by
21 centrifugation at 1,700 grams for 5 min and subsequent incubation for 48 h at 37°C with 5% CO₂.
22 The effect of the compounds on the viability of Huh-7 cells was assessed by the Alamar Blue assay
23 (Invitrogen, U.K.) according to the manufacturers protocol, followed by measurement of parasite
24 infection load by a bioluminescence assay (Biotium). Nonlinear regression analysis was employed
25 to fit the normalized results of the dose-response curves, and IC₅₀ values were determined using
26 GraphPad Prism 6.0.
27
28
29
30
31
32
33
34
35
36
37
38
39
40
41
42
43
44
45
46
47
48
49

50 **Cytotoxicity Testing:** Compounds were screened for *in vitro* cytotoxicity against Chinese
51 Hamster Ovarian (CHO) mammalian cell-lines, using the 3-(4,5-dimethylthiazol-2-yl)-2,5-
52 diphenyltetrazoliumbromide (MTT)-assay. The reference standard, emetine, was prepared to 2
53
54
55
56
57
58
59
60

1
2
3 mg/mL in distilled water while stock solutions of test compounds were prepared to 20 mg/mL in
4
5 100% DMSO with the highest concentration of solvent to which the cells were exposed having no
6
7 measurable effect on the cell viability. The initial concentration of the compounds and control was
8
9 100 µg/mL, which was serially diluted in complete medium with 10-fold dilutions to give 6
10
11 concentrations, the lowest being 0.001 µg/mL. Plates were incubated for 48 h with 100 µL of drug
12
13 and 100 µL of cell suspension in each well and developed afterwards by adding 25 µL of sterile
14
15 MTT (Thermo Fisher Scientific) to each well and followed by 4 h incubation in the dark. The
16
17 plates were then centrifuged, medium aspirated and 100 µL DMSO added to dissolve crystals
18
19 before reading absorbance at 540 nm. Data were analysed, and sigmoidal dose-response derived
20
21 using GraphPad Prism v 4.0 software (La Jolla, USA). All experiments were performed for at least
22
23 three independent biological repeats, each with technical triplicates.
24
25
26
27
28

29 **Inhibition of β -haematin Formation:** Briefly, stock solutions of control (CQ and AQ) and test
30
31 compounds were made to 20 mM in 100% DMSO. A solution containing water/305.5 µM
32
33 NP40/DMSO at a v/v ratio of 70%/20%/10%, respectively was added to every well in columns 1-
34
35 11 of a 96-well plate while 140 µL of water and 40 µL of 305.5 µM. NP40 were added to column
36
37 12 to mediate the formation of β -haematin. 20 µL of control or test compound (20 mM) was added
38
39 to column 12 and 100 µL of this solution serially diluted to column 2, with column 1 left as a blank
40
41 (0 µM compound). A 178.8 µL aliquot of haematin stock was suspended in 20 mL of a 1 M acetate
42
43 buffer, pH 4.9 and 100 µL of this haematin suspension added into each well. Plates were then
44
45 incubated for ~5 h at 37 °C after which 32 µL of pyridine solution (20% water, 20% acetone, 10%
46
47 2 M HEPES buffer pH 7.4, 50% pyridine) was added followed by addition of 60 µL of acetone to
48
49 all wells. Plates were read at 405 nm and dose-response curves plotted in GraphPad Prism v.6
50
51 (GraphPad Software Inc., La Jolla, USA) to obtain IC₅₀s values.
52
53
54
55
56
57
58
59
60

1
2
3 **Cellular heme fractionation assay:** Cultures were synchronized at 48 h intervals with 5% (w/v)
4 sorbitol, and ring-stage parasites incubated with the test drugs at various multiples of their IC₅₀s.
5
6 RBCs were then harvested after 32 h, and the trophozoites were isolated with 0.05% (wt/vol)
7
8 saponin and washed with 1× PBS (pH 7.5) to remove traces of the RBC haemoglobin. RBCs and
9
10 trophozoites were quantified in these samples using a haemocytometer and flow cytometry. The
11
12 contents of the trophozoite pellet were then released by hypotonic lysis and sonication. Following
13
14 centrifugation, the supernatants corresponding to membrane-soluble haemoglobin fraction were
15
16 treated with 4% (w/v) SDS, and 2.5% (v/v) pyridine. The pellets were again treated with 4% SDS,
17
18 25% pyridine, sonicated and centrifuged. Supernatants corresponding to the ‘free’ heme fraction
19
20 were then carefully recovered. The remaining pellets (hemozoin fraction) were then solubilized in
21
22 4% SDS, 0.3 M NaOH and then neutralized with 0.3 M HCl, sonicated, and treated with 25%
23
24 pyridine. The UV-visible spectrum of each heme fraction as an Fe(III) heme -pyridine complex
25
26 was measured using a multiwell plate reader (Spectramax 340PC; Molecular Devices). The total
27
28 amount of each heme species was quantified using a heme standard curve,¹⁶ whereby the mass of
29
30 each heme Fe species per trophozoite was calculated by dividing the total amount of each heme
31
32 species by the corresponding number of parasites in that fraction as determined by flow
33
34 cytometry.¹⁶ Statistical comparisons were made using Students t-test on GraphPad Prism 6
35
36 software (GraphPad Software Inc., La Jolla, USA).¹⁶
37
38
39
40
41
42
43
44

45 **Kinetic Solubility:** The kinetic solubility assay was performed using a miniaturized shake flask
46
47 method as previously described (Hill AP and Young RJ, 2010). Briefly, 10 mM stock solutions of
48
49 each of the compounds were used to prepare calibration standards (10-220 μM) in DMSO. The
50
51 same 10 mM stock solutions were accurately dispensed in duplicate into 96-well plates and the
52
53 DMSO dried down (MiVac GeneVac, 90 min, 37 °C). Thereafter, the samples were reconstituted
54
55
56
57
58
59
60

1
2
3 (200 μM) in aqueous solution and shaken (20 hours, 25 $^{\circ}\text{C}$). The solutions were analysed by means
4
5 of HPLC-DAD (Agilent 1200 Rapid Resolution HPLC with a diode array detector). Best fit
6
7 calibration curves were constructed using the calibration standards, which were used to determine
8
9 the aqueous solubility of the samples.
10
11

12
13 **LC-MS:** The LC purity traces were performed using one of the following methods:
14

15 **Method 1:** Using a Kinetex 2.6 μM C-18 column, 2 μL injection volume, flow 0.7 mL/min;
16
17 gradient: 15-100% B in 1.2 min (hold 3.3 min), 100-15% in 0.3 min (hold 1.2 min) (Mobile phase
18
19 A: 10 mM buffer (Ammonium acetate/acetic acid) in H_2O and Mobile phase B: 10 mM buffer
20
21 (Ammonium acetate/acetic acid) in Methanol).
22
23

24 **Method 2:** Using a Kinetex 1.7 μM C-18 column, 1 μL injection volume, flow 1.2 mL/min;
25
26 gradient: 5-100% B in 1.5 min (hold 0.4 min), 100-5% in 0.3 min (hold 0.5 min) (Mobile phase
27
28 A: 0.1% formic acid in H_2O and Mobile Phase B: 0.1% formic acid in Acetonitrile).
29
30
31

32 **Supplementary Information:** Additional details of the structures of all derivatives assessed are
33
34 provided as Supplementary material. Excel file with the compounds SMILES format is also
35
36 provided.
37
38

39 **Acknowledgements:** The University of Cape Town (KC), South African Medical Research
40
41 Council (KC, TJE, LMB and TLC), and South African Research Chairs Initiative of the
42
43 Department of Science and Technology (KC: UID 64767 and LMB: UID84627), administered
44
45 through the South African National Research Foundation, are gratefully acknowledged for support.
46
47
48

49 At Swiss TPH, we thank Christoph Fischli, Sibylle Sax and Christian for assistance in performing
50
51 the [^3H]-hypoxanthine incorporation assay.
52
53
54
55
56
57
58
59
60

REFERENCES:

- (1) W. H. O. *World Malaria Report 2017*; 2017.
- (2) Ashley, E. A.; Dhorda, M.; Fairhurst, R. M.; Amaratunga, C.; Lim, P.; Suon, S.; Sreng, S.; Anderson, J. M.; Mao, S.; Sam, B.; Sopha, C.; Chuor, C. M.; Nguon, C.; Sovannaroeth, S.; Pukrittayakamee, S.; Jittamala, P.; Chotivanich, K.; Chutasmit, K.; Suchatsoonthorn, C.; Runcharoen, R.; Hien, T. T.; Thuy-Nhien, N. T.; Thanh, N. V.; Phu, N. H.; Htut, Y.; Han, K.-T.; Aye, K. H.; Mokuolu, O. A.; Olaosebikan, R. R.; Folaranmi, O. O.; Mayxay, M.; Khanthavong, M.; Hongvanthong, B.; Newton, P. N.; Onyamboko, M. A.; Fanello, C. I.; Tshefu, A. K.; Mishra, N.; N. Valecha; Phyo, A. P.; Nosten, F.; Yi, P.; Tripura, R.; Borrmann, S.; Bashraheil, M.; Peshu, J.; Faiz, M. A.; Ghose, A.; Hossain, M. A.; Samad, R.; Rahman, M. R.; Hasan, M. M.; Islam, A.; Miotto, O.; Amato, R.; MacInnis, B.; Stalker, J.; Kwiatkowski, D. P.; Bozdech, Z.; Jeeyapant, A.; Cheah, P. Y.; Sakulthaew, T.; Chalk, J.; Intharabut, B.; Silamut, K.; Lee, S. J.; Vihokhern, B.; Kunasol, C.; Imwong, M.; Tarning, J.; Taylor, W. J.; Yeung, S.; Woodrow, C. J.; Flegg, J. A.; Das, D.; Smith, J.; Venkatesan, M.; Plowe, C. V.; Stepniewska, K.; Guerin, P. J.; Dondorp, A. M.; Day, N. P.; White, N. J. Spread of Artemisinin Resistance in Plasmodium Falciparum Malaria. *N. Engl. J. Med.* **2015**, *371* (5), 411–423. DOI:10.1056/NEJMoa1314981.
- (3) Edi, C. V. A.; Koudou, B. G.; Jones, C. M.; Weetman, D.; Ranson, H. Multiple-Insecticide Resistance in Anopheles Gambiae Mosquitoes, Southern Côte d'Ivoire. *Emerg. Infect. Dis.* **2012**, *18* (9), 1508–1511. DOI:10.3201/eid1809.120262.
- (4) Njoroge, M.; Njuguna, N. M.; Mutai, P.; Ongarora, D. S. B.; Smith, P. W.; Chibale, K. Recent Approaches to Chemical Discovery and Development against Malaria and the

- 1
2
3 Neglected Tropical Diseases Human African Trypanosomiasis and Schistosomiasis.
4
5 *Chem. Rev.* **2014**, *114* (22), 11138–11163. DOI: 10.1021/cr500098f.
6
7
8
9 (5) Chong, C. R.; Chen, X.; Shi, L.; Liu, J. O.; Sullivan, D. J. A Clinical Drug Library Screen
10 Identifies Astemizole as an Antimalarial Agent. *Nat. Chem. Biol.* **2006**, *2* (8), 415–416.
11
12 DOI: 10.1038/nchembio806.
13
14
15
16 (6) Meuldermans, W.; Hendrickx, J.; Lauwers, W.; Hurkmans, R.; Swysen, E.; Heykants, J.
17 Excretion and Biotransformation of Astemizole in Rats, Guinea-Pigs, Dogs, and Man.
18
19 *Drug Dev. Res.* **1986**, *8* (1–4), 37–51. DOI: 10.1002/ddr.430080106.
20
21
22
23
24 (7) Musonda, C. C.; Whitlock, G. A.; Witty, M. J.; Brun, R.; Kaiser, M. Chloroquine-
25 Astemizole Hybrids with Potent in Vitro and in Vivo Antiplasmodial Activity. *Bioorg.*
26
27 *Med. Chem. Lett.* **2009**, *19* (2), 481–484. DOI: 10.1016/j.bmcl.2008.11.047.
28
29
30
31
32 (8) Roman, G.; Crandall, I. E.; Szarek, W. A. Synthesis and Anti-Plasmodium Activity of
33 Benzimidazole Analogues Structurally Related to Astemizole. *ChemMedChem* **2013**, *8*
34
35 (11), 1795–1804. DOI: 10.1002/cmdc.201300172.
36
37
38
39 (9) Tian, J.; Vandermosten, L.; Peigneur, S.; Moreels, L.; Rozenski, J.; Tytgat, J.; Herdewijn,
40 P.; Van den Steen, P. E.; De Jonghe, S. Astemizole Analogues with Reduced HERG
41
42 Inhibition as Potent Antimalarial Compounds. *Bioorg. Med. Chem.* **2017**, *25* (24), 6332–
43
44 6344. DOI: 10.1016/j.bmc.2017.10.004.
45
46
47
48
49 (10) Derbyshire, E. R.; Prudencio, M.; Mota, M. M.; Clardy, J. Liver-Stage Malaria Parasites
50 Vulnerable to Diverse Chemical Scaffolds. *Proc. Natl. Acad. Sci.* **2012**, *109* (22), 8511–
51
52 8516. DOI: 10.1073/pnas.1118370109.
53
54
55
56
57
58
59
60

- 1
2
3 (11) Van der Zee, J.; Barr, D. P.; Mason, R. P. ESR Spin Trapping Investigation of Radical
4 Formation from the Reaction between Hematin and Tert-Butyl Hydroperoxide. *Free*
5 *Radic. Biol. Med.* **1996**, *20* (2), 199–206. DOI: 10.1016/0891-5849(95)02031-4
6
7
8
9
10
11 (12) Schmitt, T. H.; Frezzatti, W. A.; Schreier, S. Hemin-Induced Lipid Membrane Disorder
12 and Increased Permeability: A Molecular Model for the Mechanism of Cell Lysis. *Arch.*
13 *Biochem. Biophys.* **1993**, *307* (1), 96–103. DOI: 10.1006/abbi.1993.1566.
14
15
16
17
18 (13) Ploemen, I. H. J.; Prudêncio, M.; Douradinha, B. G.; Ramesar, J.; Fonager, J.; Van
19 Gemert, G. J.; Luty, A. J. F.; Hermsen, C. C.; Sauerwein, R. W.; Baptista, F. G.; Mota, M.
20 M.; Waters, A. P.; Que, I.; Lowik, C. W. G. M.; Khan, S. M.; Janse, C. J.; Franke-Fayard,
21 B. M. D. Visualisation and Quantitative Analysis of the Rodent Malaria Liver Stage by
22 Real Time Imaging. *PLoS One* **2009**, *4* (11), 1–12. DOI: 10.1371/journal.pone.0007881.
23
24
25
26
27
28
29
30
31 (14) Mann, K. V; Crowe, J. P.; Tietze, K. J. Nonsedating Histamine H1-Receptor Antagonists.
32 *Clin. Pharm.* **1989**, *8* (5), 331–344.
33
34
35
36
37 (15) Ncokazi, K. K.; Egan, T. J. A Colorimetric High-Throughput Beta-Hematin Inhibition
38 Screening Assay for Use in the Search for Antimalarial Compounds. *Anal. Biochem.* **2005**,
39 *338* (2), 306–319. DOI: 10.1016/j.ab.2004.11.022.
40
41
42
43
44 (16) Combrinck, J. M.; Fong, K. Y.; Gibhard, L.; Smith, P. J.; Wright, D. W.; Egan, T. J.
45 Optimization of a Multi-Well Colorimetric Assay to Determine Haem Species in
46 Plasmodium Falciparum in the Presence of Anti-Malarials. *Malar. J.* **2015**, *14*, 253. DOI:
47 10.1186/s12936-015-0729-9.
48
49
50
51
52
53
54 (17) Snyder, C.; Chollet, J.; Santo-Tomas, J.; Scheurer, C.; Wittlin, S. In Vitro and in Vivo
55
56
57
58
59
60

- 1
2
3 Interaction of Synthetic Peroxide RBx11160 (OZ277) with Piperaquine in Plasmodium
4 Models. *Exp. Parasitol.* **2007**, *115* (3), 296–300. DOI: 10.1016/j.exppara.2006.09.016.
5
6
7
8
9 (18) Dorn, A.; Stoffel, R.; Matile, H.; Bubendorf, A.; Ridley, R. G. Malarial Haemozoin/Beta-
10 Haematin Supports Haem Polymerization in the Absence of Protein. *Nature* **1995**, *374*
11 (6519), 269–271. DOI: 10.1038/374269a0.
12
13
14
15
16 (19) Trager, W.; Jensen, J. B. Human Malaria Parasites in Continuous Culture. *Science* **1976**,
17 *193* (4254), 673–675. DOI: 10.1126/science.781840.
18
19
20
21
22 (20) Huber, W.; Koella, J. C. A Comparison of Three Methods of Estimating EC50 in Studies
23 of Drug Resistance of Malaria Parasites. *Acta Trop.* **1993**, *55* (4), 257–261.
24
25
26 DOI: 0.1016/0001-706X(93)90083-N.
27
28
29 (21) Reader, J.; Botha, M.; Theron, A.; Lauterbach, S. B.; Rossouw, C.; Engelbrecht, D.;
30 Wepener, M.; Smit, A.; Leroy, D.; Mancama, D.; Coetzer, T. L.; Birkholtz, L. Nowhere to
31 Hide: Interrogating Different Metabolic Parameters of Plasmodium Falciparum
32 Gametocytes in a Transmission Blocking Drug Discovery Pipeline towards Malaria
33 Elimination. *Malar. J.* **2015**, *14* (1), 213. DOI: 10.1186/s12936-015-0718-z.
34
35
36
37
38
39
40
41
42
43
44
45
46
47
48
49
50
51
52
53
54
55
56
57
58
59
60

For Table of Contents Use Only